

ADA036715

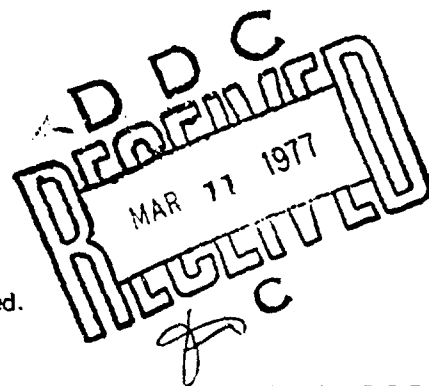
TECHNICAL REPORT RD-77-4

THE AERODYNAMIC CHARACTERISTICS OF WRAP-AROUND
FINS AT MACH NUMBERS OF 0.3 TO 3.0

C. Wayne Dahlke
Aeroballistics Directorate
US Army Missile Research, Development and Engineering Laboratory
US Army Missile Command
Redstone Arsenal, Alabama 35809

15 October 1976

Cleared for public release; distribution unlimited.



U.S. ARMY MISSILE COMMAND

Redstone Arsenal, Alabama

DISPOSITION INSTRUCTIONS

**DESTROY THIS REPORT WHEN IT IS NO LONGER NEEDED. DO NOT
RETURN IT TO THE ORIGINATOR.**

DISCLAIMER

**THE FINDINGS IN THIS REPORT ARE NOT TO BE CONSTRUED AS AN
OFFICIAL DEPARTMENT OF THE ARMY POSITION UNLESS SO DESIGNATED
BY OTHER AUTHORIZED DOCUMENTS.**

TRADE NAMES

**USE OF TRADE NAMES OR MANUFACTURERS IN THIS REPORT DOES
NOT CONSTITUTE AN OFFICIAL INDORSEMENT OR APPROVAL OF
THE USE OF SUCH COMMERCIAL HARDWARE OR SOFTWARE.**

UNCLASSIFIED

SECURITY CLASSIFICATION OF THIS PAGE (When Data Entered)

REPORT DOCUMENTATION PAGE		READ INSTRUCTIONS BEFORE COMPLETING FORM	
1. REPORT NUMBER RD-77-4	2. GOVT ACCESSION NO.	3. RECIPIENT'S CATALOG NUMBER	
4. TITLE (and Subtitle) THE AERODYNAMIC CHARACTERISTICS OF WRAP-AROUND FINS AT MACH NUMBERS OF 0.3 TO 3.0.		5. TYPE OF REPORT & PERIOD COVERED Technical Report.	
7. AUTHOR(s) C. Wayne Dahlke		6. PERFORMING ORG. REPORT NUMBER	
9. PERFORMING ORGANIZATION NAME AND ADDRESS Commander US Army Missile Command Attn: DRSMI-RD Redstone Arsenal, Alabama 35809		8. CONTRACT OR GRANT NUMBER(s)	
11. CONTROLLING OFFICE NAME AND ADDRESS Commander US Army Missile Command Attn: DRSMI-RPR Redstone Arsenal, Alabama 35809		10. PROGRAM ELEMENT, PROJECT, TASK AREA & WORK UNIT NUMBERS (DA) 1W362303A214 AMCMSC 632303.2140511.05	
14. MONITORING AGENCY NAME & ADDRESS (if different from Controlling Office)		12. REPORT DATE 15 Oct 1976	
		13. NUMBER OF PAGES 63 p.	
		15. SECURITY CLASS. (of this report) Unclassified	
		15a. DECLASSIFICATION/DOWNGRADING SCHEDULE	
16. DISTRIBUTION STATEMENT (of this Report) Cleared for public release; distribution unlimited.			
17. DISTRIBUTION STATEMENT (of the abstract entered in Block 20, if different from Report)			
18. SUPPLEMENTARY NOTES			
19. KEY WORDS (Continue on reverse side if necessary and identify by block number) Wrap-around fin Geometric and flow parameters Static stability Dynamic stability Drag			
20. ABSTRACT (Continue on reverse side if necessary and identify by block number) Results of investigations into many of the geometric and flow parameters influencing the aerodynamics of wrap-around fins are presented in this report. Particular emphasis is placed on defining static and dynamic roll characteristics between Mach numbers of 0.3 to 3.0. Among the geometric parameters highlighted are fin span, aspect ratio, leading edge sweep, leading edge shape, fin opening angle, and afterbody geometry. Comparisons of static stability, dynamic stability, and drag are made between the flat and the wrap-around fin.			

DD FORM 1 JAN 73 1473

EDITION OF 1 NOV 65 IS OBSOLETE

UNCLASSIFIED

SECURITY CLASSIFICATION OF THIS PAGE (When Data Entered)

444467

Dahlke

UNCLASSIFIED

SECURITY CLASSIFICATION OF THIS PAGE (When Data Entered)

Block 20 (Concluded)

Problems associated with measurement of wrap-around fin rolling mounts are also discussed. An overview of the wrap-around fin roll moment characteristics are presented as an aid for making estimates and establishing testing techniques. This report supercedes RD-73-17.

ACCESSION for	White Section	<input checked="checked" type="checkbox"/>
NTIS	Buff Section	<input type="checkbox"/>
DDC		
UNCLASSIFIED		
JUSTIFICATION		
BY	DISTRIBUTION AVAILABILITY CODES	
DATE	SPECIAL	
<i>A</i>		

UNCLASSIFIED

SECURITY CLASSIFICATION OF THIS PAGE (When Data Entered)

CONTENTS

	Page
I. INTRODUCTION.	3
II. MODELS AND EXPERIMENTAL TEST.	3
III. TESTING TECHNIQUES AND ACCURACY	5
IV. COMPARISON OF WAF TO FLAT FIN STABILITY AND DRAG. . . .	15
V. ROLLING MOMENT COEFFICIENT.	16
VI. SIDE FORCES AND MOMENTS	36
VII. OPENING ANGLE	36
VIII. WAF ROLL DYNAMICS	45
IX. CONCLUSIONS	51
SYMBOLS	53
REFERENCES.	55
BIBLIOGRAPHY.	57

I. INTRODUCTION

The wrap-around fin (WAF) may be used in many applications to provide missile performance equal to flat fins. The WAF has had limited use as stabilizing surfaces, and has been considered for use as control surfaces.

One of the main thrust of modern military technology is accuracy improvement for the most basic form of missilery, the free flight rocket. Both existing free flight rockets and future concepts range from large fixed and/or vehicle launched, to sizes and weights small enough to be man-portable and shoulder fired. The stabilizing surfaces may be constrained by physical limitations imposed by rocket motor geometry and launcher considerations.

The WAF offers a solution for many geometric constraints, and in many applications can be sized to provide aerodynamic stabilizing characteristics equal to flat fin stabilizers. The WAF, however, has unique aerodynamic characteristics, particularly in roll, that are different from other types of stabilizing devices. The WAF is inherently adaptable to tube launched constraints, making it, perhaps, the most practical for tube launched rockets.

This report contains a summary of the findings from wind tunnel tests conducted by the US Army Missile Command (MICOM), Redstone Arsenal, Alabama, with partial support provided by the Air Force Armament Test Labs (AFATL). The ultimate goal is to develop an analytical model to describe the flow phenomena defining the unique WAF aerodynamic forces; however, at the time, because of the need, it was more expedient to define the characteristics through systematic parameteric wind tunnel test. The objective of this study was to uncover characteristics and provide trends that can be used in missile design where the analytical models are not available. The results from this study and other data, such as the Navy [1] pressure data, should provide sufficient information to begin development of an analytical model. The data herein are presented for comparison of several of the parameters, with important characteristics and trends highlighted, illustrating those that have the most significant effect upon the WAF rolling moment coefficient. Problems associated with measurement of WAF roll moment coefficients using conventional techniques are mentioned. In addition to references cited in this report, a bibliography of other WAF documents is included.

II. MODELS AND EXPERIMENTAL TEST

MICOM and AFATL undertook the study of fins and afterbody geometric effects on the static rolling moment characteristics of WAF, as agreed to in the initial planning of a TTCF cooperative program. Fin geometry was varied around the standard WAF (F1, Table 1) shown in

TABLE 1. FIN CONFIGURATION SUMMARY

Configuration	A (in.)	C _R (in.)	$\frac{C_T}{C_R}$	A (deg)	t (in.)	R ₁ (in.)	R ₂ (in.)	R ₃ (in.)	δ* (deg)	r (in.)	AR	b/2 (in.)
F1**	1.900	7.0	1.00	0	0.200	1.900	2.000	1.800	45	0.008	0.75	2.64
F2	1.900	4.0	1.00	1.00	0.114	1.900	1.957	1.843	45	1.30	1.30	2.60
F3	1.900	2.0	1.00	0.057	0.057	1.900	1.929	1.871	45	2.60	2.60	2.60
F4	1.900	7.0	1.00	0.200	0.200	1.900	2.000	1.800	①	0.76	0.76	2.64
F5	1.900	4.0	1.00	0.200	0.200	1.900	2.000	1.800	20	0.76	0.76	2.64
F6	1.900	2.0	1.00	0.200	0.200	1.900	2.000	1.800	②	0.76	0.76	2.64
F7	1.900	7.0	1.00	0.107	0.107	1.900	1.953	1.847	45	0.76	0.76	2.64
F8	1.900	4.0	1.00	0.315	0.315	1.900	2.058	1.743	45	0.76	0.76	2.64
F9	2.000	7.0	1.00	0.200	0.200	2.000	2.058	1.743	45	0.75	0.75	2.64
F10 ④	1.900	7.0	1.00	0	0.200	1.900	2.000	1.800	45	0.008	0.40	1.39
F11	Fin "F1" with tip chord modified											
F12	1.900	7.0	0.9	14.75	0.200	1.900	2.000	1.800	45	0.73	0.73	2.59
F13	1.900	4.0	0.75	33.9	0.200	1.900	2.000	1.800	45	0.79	0.79	2.63
F14	1.900	2.0	0.60	46.9	0.200	1.900	2.000	1.800	45	0.86	0.86	2.63
F15	1.900	7.0	1.00	0	0.040	1.900	1.900	1.860	45	0.94	0.94	2.63
F16	1.900	4.0	0.75	20.6	0.114	1.900	2.000	1.800	45	1.32	1.32	2.65
F17	1.900	2.0	0.36	60.0	0.200	1.900	2.000	1.800	45	1.54	1.54	2.70
F18	1.900	7.0	0.33	46.9	0.120	1.900	2.000	1.800	45	1.11	1.11	2.63
F19	1.900	4.0	0.00	57.3	0.120	1.900	2.000	1.800	45	1.97	1.97	2.61
F20	1.900	7.0	1.00	0	0.200	1.900	2.000	1.800	45	2.55	2.55	2.55
F21	1.900	7.0	1.00	0	0.200	1.900	2.000	1.800	45	0.61	0.61	2.14

*Leading edge angle. All trailing edges δ = 45°.

**Standard TTCP WAF.

- ① Blunt leading edge.
- ② Unsymmetrical leading edge.
- ③ Rectangular flat planform, exposed span = 2.658 in.
- ④ Cap fin.
- ⑤ Tip chord parallel to root chord.

the Arnold Engineering Development Center's (AEDC) 4-T wind tunnel in Figure 1. The models consisted of a 2-caliber secant ogive nose with an 8-caliber cylindrical afterbody, including 3 afterbody shapes and fin configurations. The basic body configuration had a straight cylindrical afterbody (4 inches in diameter) and two alternate afterbody shapes stepped down to a diameter of 3.6 inches over a length of 7 and 4 inches, respectively, from the base (Figure 2).

The exposed semispan $b/2$ for the WAF was chosen to be approximately the chord length for the arc that encloses a quadrant of tubular body cross section or $0.707 D$ (Figure 3 and Table 1). These variations (Table 1) included two larger aspect ratios (same span as standard WAF with shorter chords of 2 and 4 inches), three additional thickness ratios, four leading edge shapes, seven leading edge sweep angles, one tip alteration, two reduced span fins, one fin body gap, and several of these fins tested on a step down body configuration (Figure 2). An investigation of fin opening/closing angle for the standard WAF was conducted for seven opening positions ranging from fully closed to 10° beyond the standard fully opened case. Static aerodynamic measurements, including total airframe and individual fin force and moment characteristics, were conducted in three wind tunnel facilities. The majority of transonic tests were conducted in the AEDC 4-foot transonic wind tunnel [2,3,4,5,6], while the majority of supersonic tests were conducted in the NASA Langley 4-foot unitary plan wind tunnel [7]. Limited transonic and supersonic tests were conducted in the McDonnell Douglas Aerophysics 4-foot trisonic wind tunnel [8]. In addition, limited roll damping characteristics were conducted in the AEDC 4-foot transonic facility [9], and both subsonic and supersonic free flight tests were conducted in the Jet Propulsion Laboratory (JPL) 20-inch supersonic wind tunnel for the standard WAF configuration and its equivalent planar fin, F9 (Figure 4). Test variables for the static aerodynamic tests are listed in Table 2 for the varying geometry tests. In addition to these MICOM/AFATL sponsored tests to specifically study the WAF effects, several projects have considered use of the WAF; some are listed by Holmes [1] and others are briefly mentioned in this report. A more complete description of the models and testing conducted by MICOM is contained in data reports [2,3,5,6,7].

III. TESTING TECHNIQUES AND ACCURACY

There are questions concerning the accuracy and repeatability of the rolling moment coefficient data. The magnitudes of the self-induced rolling moment coefficients of the WAF are small in relation to the size of the coefficients of fins with large cant. The only ready means of obtaining force data in a wind tunnel is with a strain gage balance. The balance must be sized to meet special requirements, but it must be capable of handling the forces and moments of the complete model in the test facility to be used. To obtain sensible rolling moment coefficients induced by WAF, wind tunnel dynamic pressure and fin sizes must be made large within practicable limits. Both cause

TABLE 2. SUMMARY OF WAF STATIC TEST

CONFIGURATION	0.3	0.5	0.6	0.7	0.8	0.9	0.95	1.0	1.05	1.1	1.2	1.3	1.6	1.9	2.0	2.36	2.5	2.86	3.0
B1	●	●	●	●	●	●	●	●	●	●	●	●	●	●	●	●	●	●	●
B1F1	●	●	●	●	●	●	●	●	●	●	●	●	●	●	●	●	●	●	●
B1F2	●	●	●	●	●	●	●	●	●	●	●	●	●	●	●	●	●	●	●
B1F3	●	●	●	●	●	●	●	●	●	●	●	●	●	●	●	●	●	●	●
B1F4	●	●	●	●	●	●	●	●	●	●	●	●	●	●	●	●	●	●	●
B1F5	●	●	●	●	●	●	●	●	●	●	●	●	●	●	●	●	●	●	●
B1F6	●	●	●	●	●	●	●	●	●	●	●	●	●	●	●	●	●	●	●
B1F7	●	●	●	●	●	●	●	●	●	●	●	●	●	●	●	●	●	●	●
B1F8	●	●	●	●	●	●	●	●	●	●	●	●	●	●	●	●	●	●	●
B1F9	●	●	●	●	●	●	●	●	●	●	●	●	●	●	●	●	●	●	●
B1F10	●	●	●	●	●	●	●	●	●	●	●	●	●	●	●	●	●	●	●
B1F11	●	●	●	●	●	●	●	●	●	●	●	●	●	●	●	●	●	●	●
B1F12	●	●	●	●	●	●	●	●	●	●	●	●	●	●	●	●	●	●	●
B1F13	●	●	●	●	●	●	●	●	●	●	●	●	●	●	●	●	●	●	●
B1F14	●	●	●	●	●	●	●	●	●	●	●	●	●	●	●	●	●	●	●
B1F15	●	●	●	●	●	●	●	●	●	●	●	●	●	●	●	●	●	●	●
B1F16	●	●	●	●	●	●	●	●	●	●	●	●	●	●	●	●	●	●	●
B1F17	●	●	●	●	●	●	●	●	●	●	●	●	●	●	●	●	●	●	●
B1F18	●	●	●	●	●	●	●	●	●	●	●	●	●	●	●	●	●	●	●
B1F19	●	●	●	●	●	●	●	●	●	●	●	●	●	●	●	●	●	●	●
B1F20	●	●	●	●	●	●	●	●	●	●	●	●	●	●	●	●	●	●	●
B1F21	●	●	●	●	●	●	●	●	●	●	●	●	●	●	●	●	●	●	●
B2	●	●	●	●	●	●	●	●	●	●	●	●	●	●	●	●	●	●	●
B2F1	●	●	●	●	●	●	●	●	●	●	●	●	●	●	●	●	●	●	●
B2F10	●	●	●	●	●	●	●	●	●	●	●	●	●	●	●	●	●	●	●
B2F13	●	●	●	●	●	●	●	●	●	●	●	●	●	●	●	●	●	●	●
B3F2	●	●	●	●	●	●	●	●	●	●	●	●	●	●	●	●	●	●	●
B3F16	●	●	●	●	●	●	●	●	●	●	●	●	●	●	●	●	●	●	●

○ TC 154/170 (REF 2)

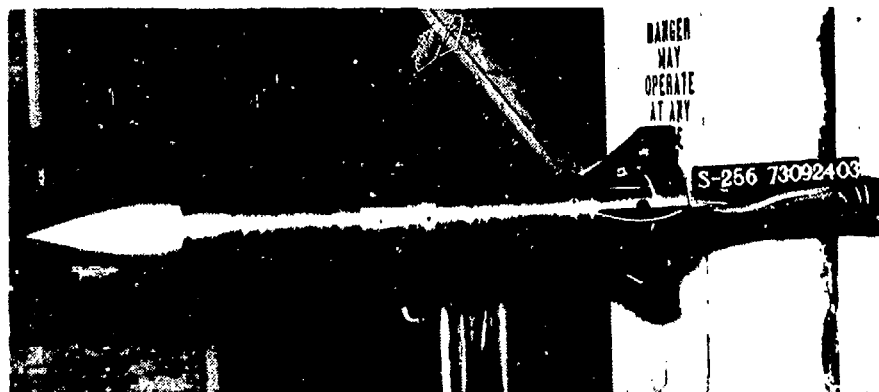
◇ UPWT 980 (REF 7)

△ TC 273 (REF 3)

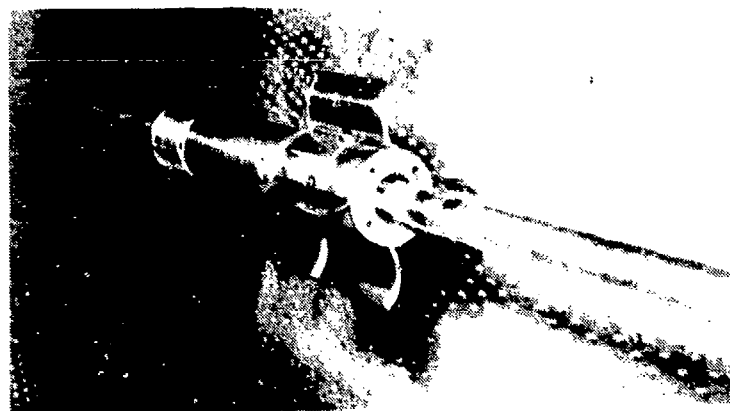
□ TC 202 (REF 5)

□ S-256 (REF 8)

SOLID SYMBOLS: ZERO ROLL ANGLE ONLY



MODEL INSTALLATION STANDARD CONFIGURATION, $\phi = 0$, $\alpha = 0$



SWEPT FIN CONFIGURATION



SPLITTER PLATE

Figure 1. WAF model.

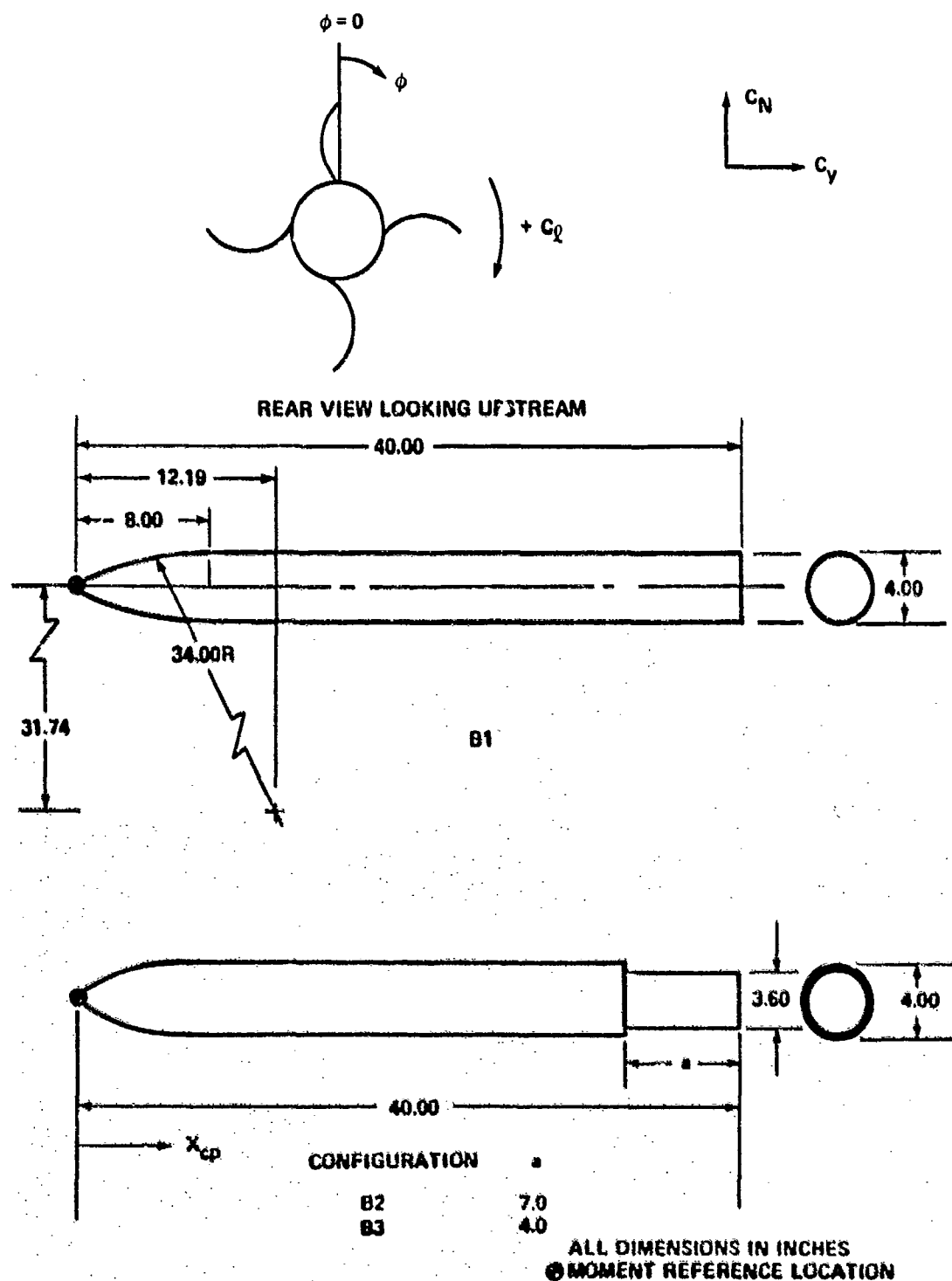


Figure 2. External body geometry.

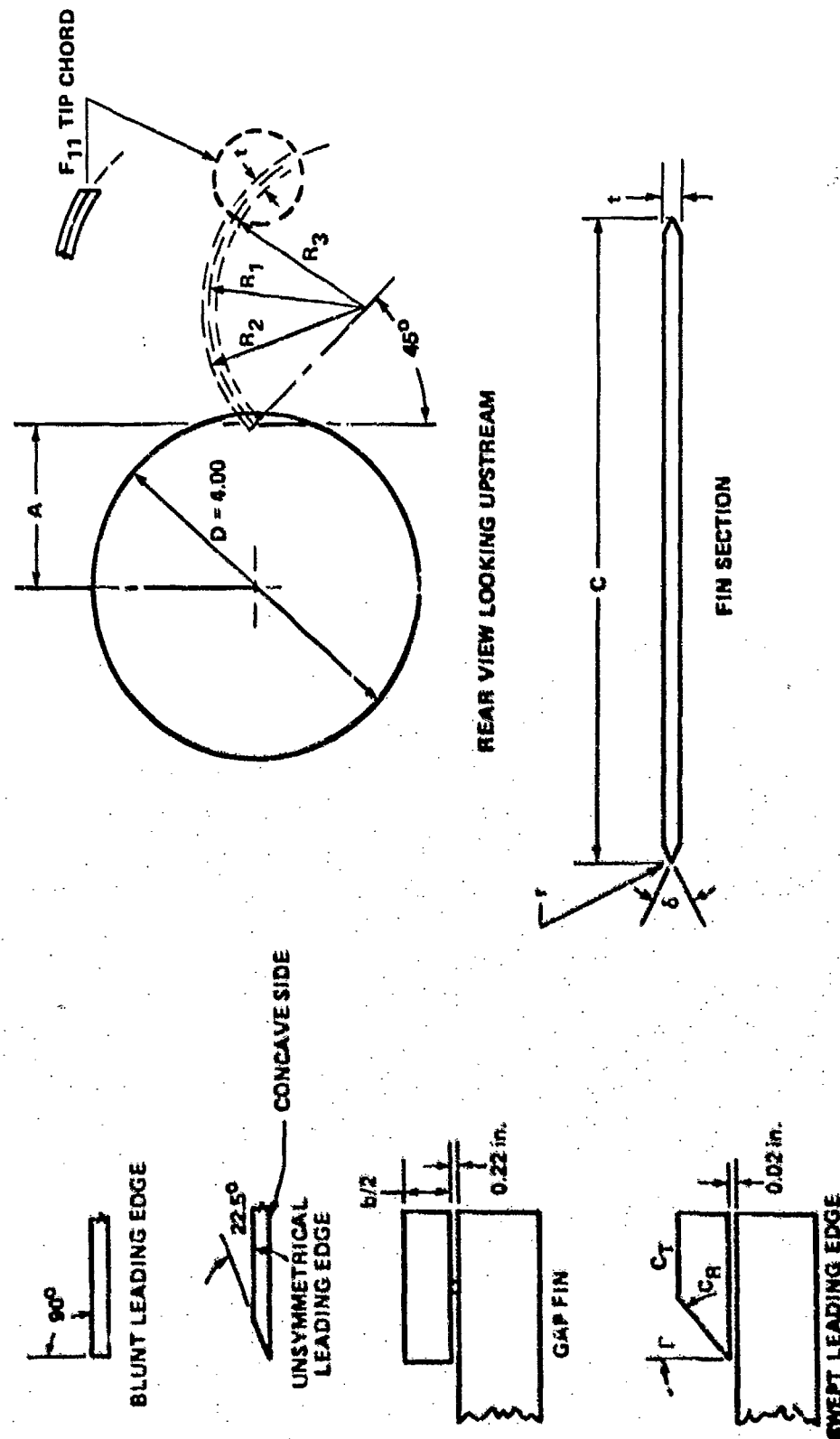


Figure 3. WAF geometry.



Figure 4. JPL free flight models.

larger aerodynamic loads on the model which result in requirements of larger strain gage balances. To date, strain gage balances and associated instrumentation are not ideal for measurement of these small rolling moments; however, from the available balances one can be chosen that is optimum for given requirements. A composite plot of rolling moment data precision is shown in Figure 5. At transonic speeds, the rolling moment gage was large because of the requirements dictated by normal force and pitching moment loads. As a result the data precision, as quoted by AEDC [3,5], is larger than desirable; however, as shown later, the repeatability from duplicate points during the same test and from separate entries show that the data are reproducible well within these precision limits. An attempt was made to measure the cant of each fin during the transonic testing [2,5]. These measurements of 76 fin installations had a mean cant of 0.011° with a standard deviation of 0.142° , with a quoted measurement accuracy of $\pm 0.1^\circ$. If all four fins for one configuration have a 0.1° cant, the rolling moment coefficient would be 0.004 to 0.010 which is within the quoted (Figure 5) data precision for the subsonic/transonic test. Because of the uncertainty of the cant measurements and the small magnitude of fin cant-induced rolling moment relative to the data precision, corrections to rolling moment coefficient caused by fin cant are not presented.

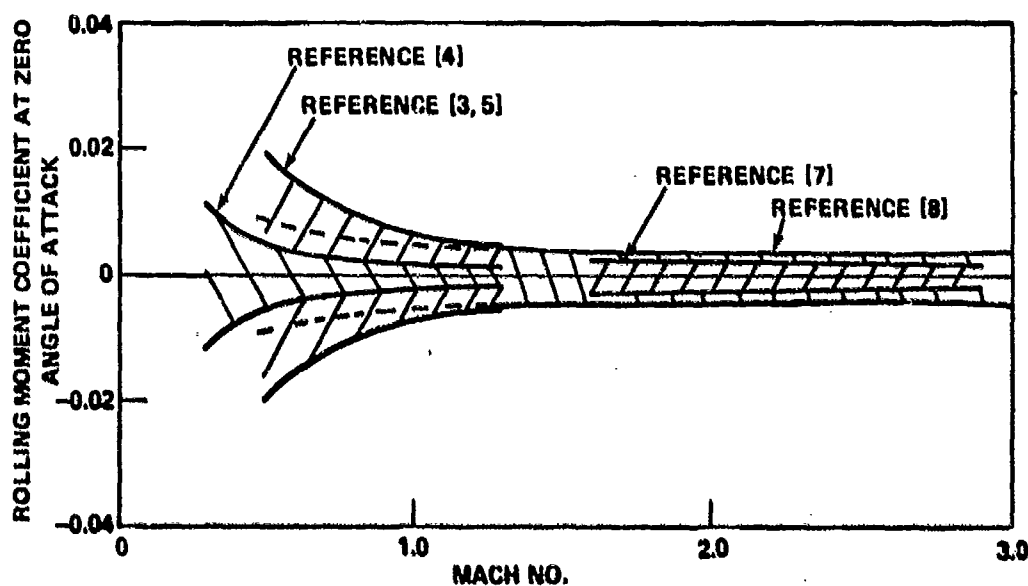


Figure 5. WAF rolling moment data precision.

Several comparisons were made from the numerous duplications and other geometric similarities. Figure 6 shows a comparison of the 1-caliber chord WAF configuration B1F2 tested on the smooth body with four main balances and in three different facilities. A separate test [4] was conducted explicitly to check the rolling moment obtained in

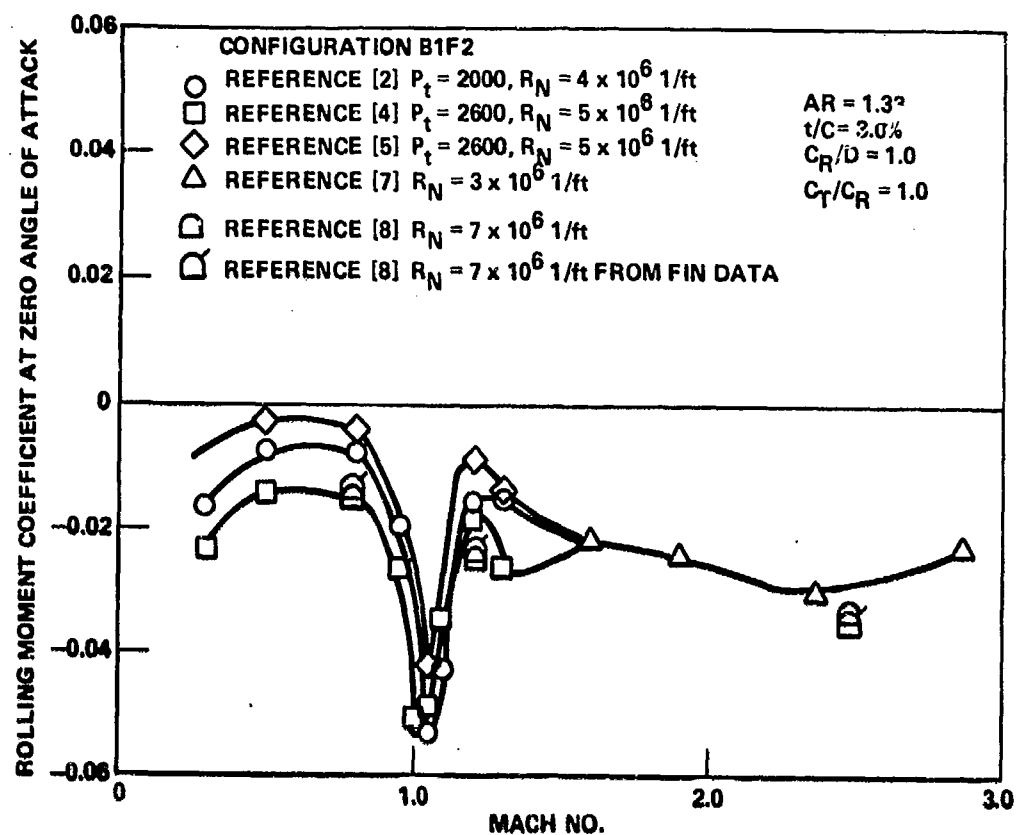


Figure 6. WAF rolling moment coefficient comparisons from several tests, $\alpha = 0$, $\phi = 0$.

an earlier test [2] at transonic speeds. This test was conducted with a balance that had a 100-inch-pound roll moment gage. The normal force and pitching moment gages were also low capacity, and angle of attack was restricted to less than 2° . The main purpose of this test was to observe the self-induced WAF rolling moment coefficient at zero angle of attack, and compare these to previously obtained coefficients with the less sensitive balance. Comparisons of this repeat test are shown in Figure 6 by the square symbol.

Most models were tested at 0° and 45° roll angles (Figure 2) throughout the Mach number range at angles of attack of -6° to 6° . The outcome of the rolling moment coefficient should be the same for any roll angle at zero angle of attack from a flow and model symmetry viewpoint. Differences between roll position can be attributed to data instrumentation repeatability. Figure 7 shows self-induced WAF rolling moment coefficients at zero angle of attack throughout the Mach number range for two roll angles of 0° and 45° . This does not necessarily indicate the precision of the data, but these results are typical of the repeatability of the data for both the transonic and supersonic

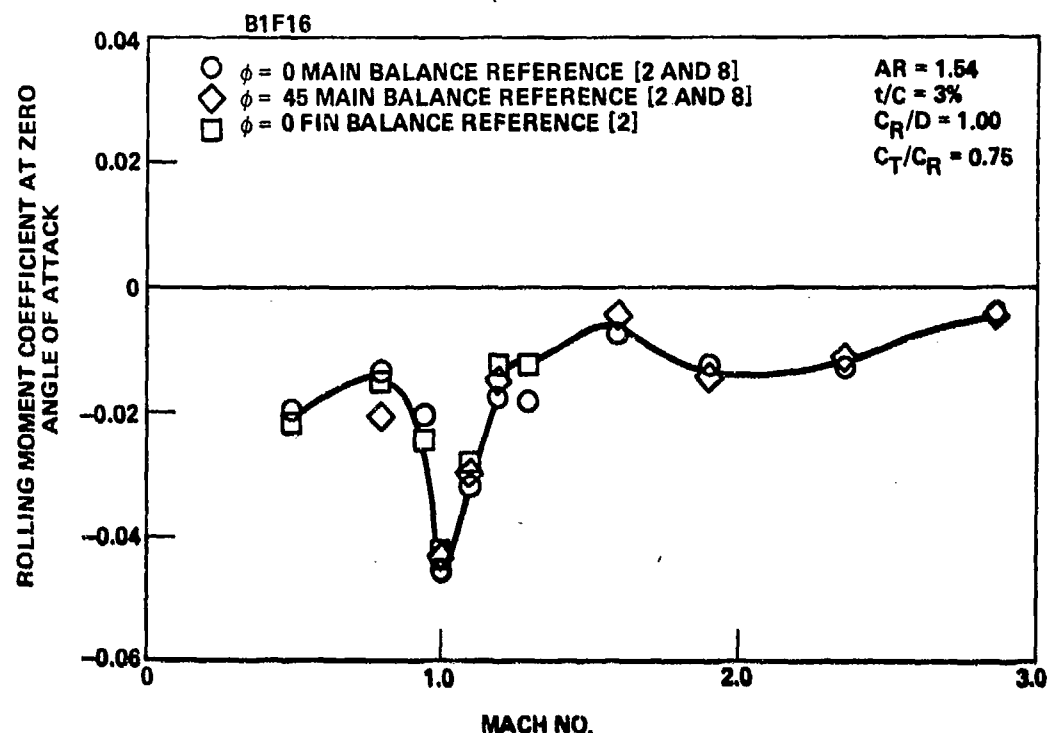


Figure 7. WAF roll moment coefficient from main balance and fin balances, $\phi = 0$ and 45 degrees.

phases of testing. Tests were conducted for other roll angles during the transonic phase, and all results were compatible with those shown in Figure 7.

Each fin was mounted on a three component strain gage balance. Total missile rolling moment coefficient was computed from the measured fin normal force and root bending moment coefficient and compared to the rolling moment coefficient obtained from the main balance. Typical comparisons of the WAF self-induced rolling moment coefficient at zero angle of attack for the transonic test are shown in Figure 8. The data most questionable are the transonic phase, as shown in Figure 5, where comparison between the two methods of obtaining rolling moment coefficient are better than expected.

In addition to the computed rolling moment coefficient from the four fin panel balances, shown by the flagged symbols (Figure 8), the rolling moment coefficient also includes the main balance data for the TTCF standard WAF B1 F1. Fin cant variation can produce roll moments equally as large as any WAF-induced roll moment observed during all tests. Superimposed on the data of Figure 8 is the roll moment coefficient for a typical tactical prototype fin with incidence (cant) tolerance of 0.1° for all four fins, where the nominal fin incidence was zero. The overall value of this analysis is to indicate the

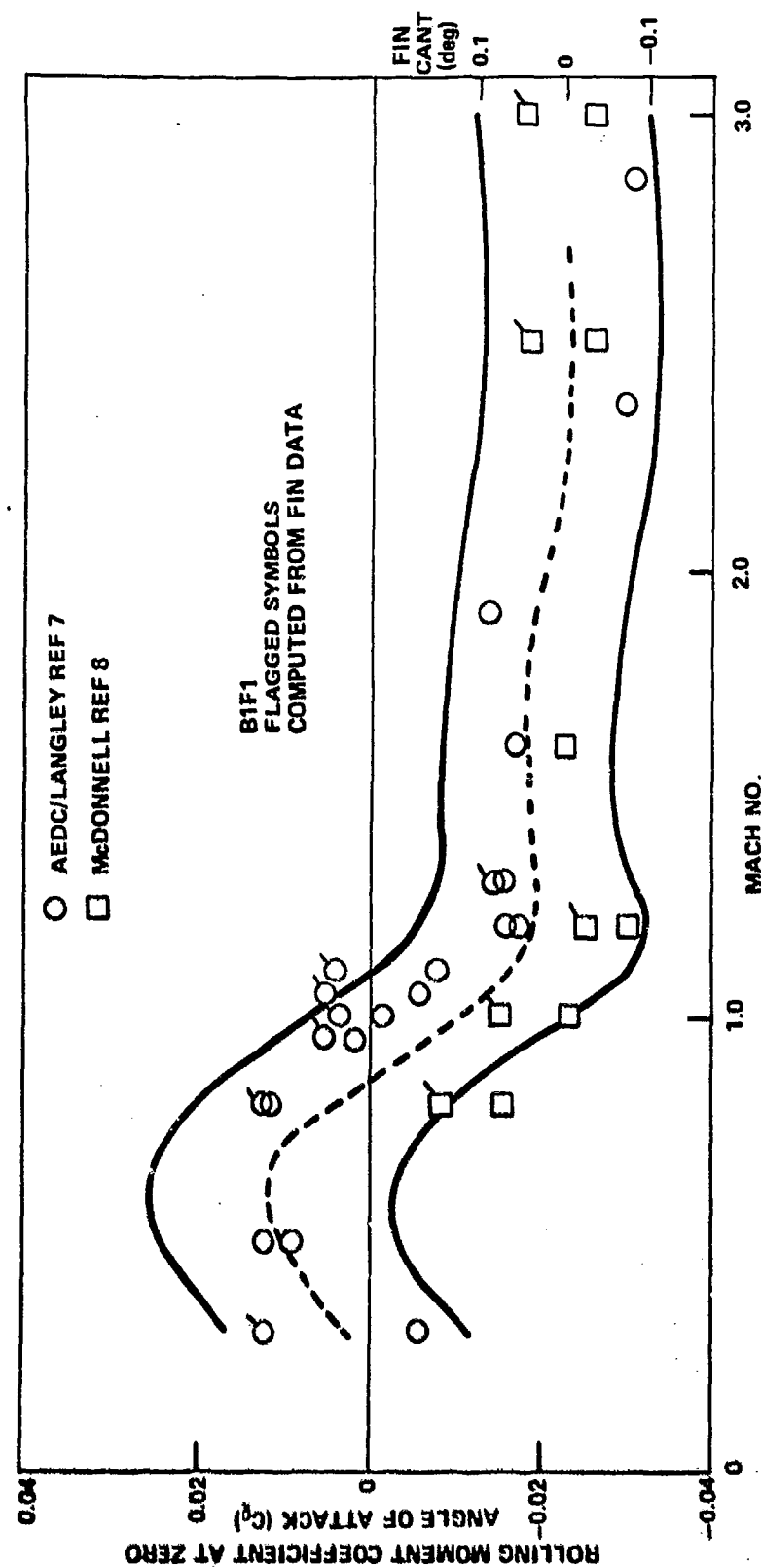


Figure 8. Comparison of data scatter to fin cant tolerance.

difficulty in obtaining the precise magnitudes that a WAF may exhibit with flight hardware; however, the trends shown here and those in the following sections are realistic. To obtain the accuracy of the magnitudes desired will require extreme care in model fabrication and sophisticated measurement techniques tailored for precise roll moment measurement.

IV. COMPARISON OF WAF TO FLAT FIN STABILITY AND DRAG

The major concern of the effects of WAF has been the self-induced rolling moment; however, additional comparison of static stability parameters was made for a flat fin and the standard WAF. The flat fin had the same total exposed span and projected area as the WAF. These two fins were tested through the Mach number range of 0.3 to 3.0 on a body of revolution. The normal force coefficient slope at zero angle of attack and the center of pressure are shown in Figure 9 for the flat fin and WAF. Any difference in total configuration static stability coefficients appears to be within the uncertainty of measurement accuracy. Included on the center of pressure data are points from the JPL free flight bi-planar results at Mach 0.86, 2.0, and 3.03. Similar results were obtained from a comparison of data for the flat fin and WAF tested on a reflection plane at transonic speeds and from body mounted fin panel data. The flat fin and WAF were also compared by testing both on a reflection plane [6] (Figure 1, bottom photo) at transonic speeds. Figure 10 shows the basic WAF and flat fin coefficient variations with angle of attack for Mach 0.3 to 1.3. This shows that the basic lifting characteristic of the WAF is essentially the same as the flat fin for angles of attack less than 4° . Figure 11 shows the flat and WAF basic fin lift curve slope at zero angle of attack along with the longitudinal and lateral center of pressure for the fin on a flat plate and on the body of revolution. The only significant difference between the splitter plate data and the data for fins on the body of revolution is the increase in normal force coefficient caused by body upwash. The upwash factor obtained from the ratio of these two curves ranges from 1.4 to 1.7 through the Mach range of 0.3 to 1.3. This is comparable to the slender body theory factor of 1.39 for this fin with a body diameter to total span ratio of 0.43.

Drag coefficient comparisons between the flat and WAF configurations are shown on Figure 12. The upper portion shows the drag force coefficient for body alone, the WAF and body, and the flat fin (of equal projected area to the WAF) and body. The lower portion shows the same data with the body alone, drag subtracted out. The WAF is approximately 10% higher, which corresponds to the additional frontal area that the WAF has because of the curvature. The other geometric parameters (leading edge sweep, thickness, leading edge shape, and aspect ratio) show their influence on drag to be as expected for flat fins with the same geometric changes.

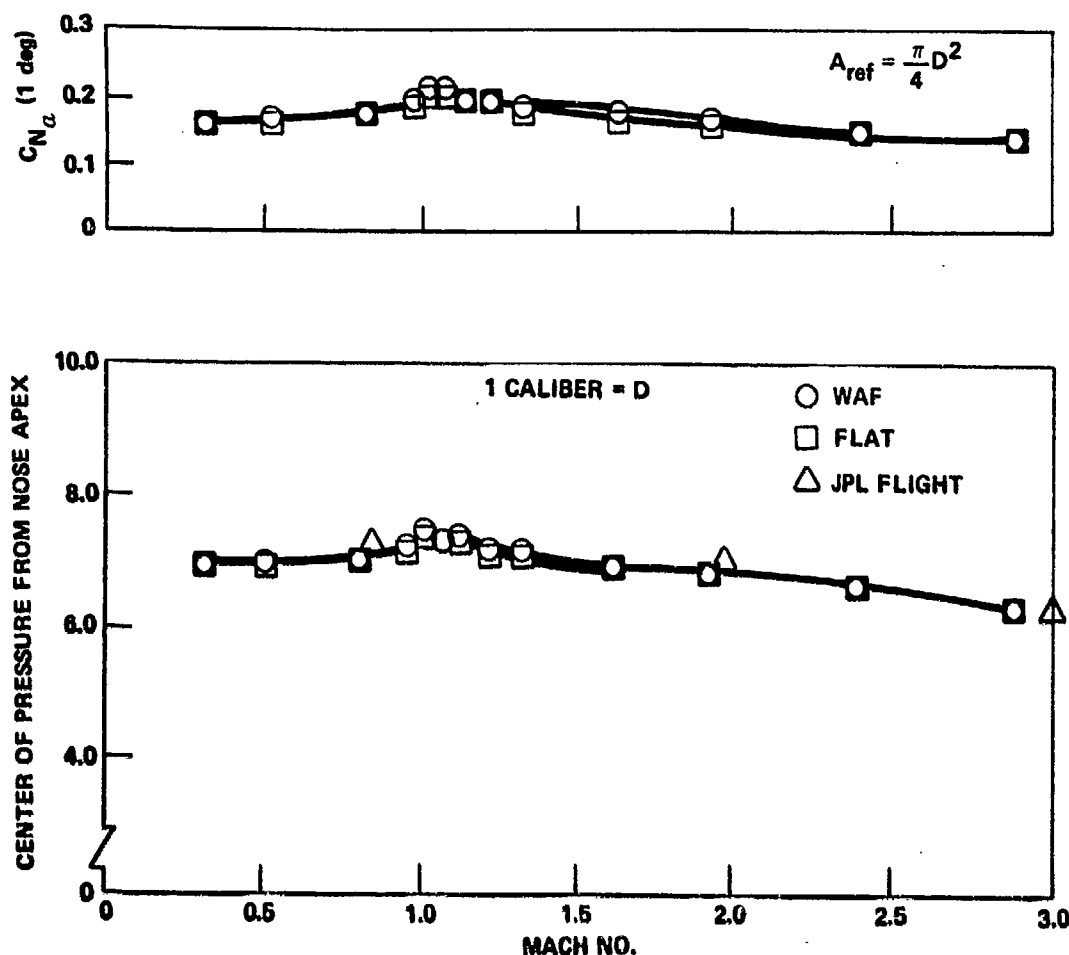


Figure 9. Comparison of flat and WAF static stability derivatives.

V. ROLLING MOMENT COEFFICIENT

The main objective for this study was to investigate the effects on WAF rolling moment due to the various geometric and flow parameters. The variation of rolling moment is considered for three flow parameters: Mach number, Reynolds number, and angle of attack for several geometric variations. Featherstone and Dahlke [10,11] have shown the WAF to have self-induced normal forces at zero angle of attack. The most significant effect with Mach number appears to be at transonic speeds where, in general, a change in sign occurs for rolling moment. In initial studies, Featherstone has suggested the self-induced force is directed toward the center of curvature at subsonic speeds and away from the center of curvature at supersonic speeds with the crossover occurring close to Mach = 1. This was demonstrated for those fin configurations on smooth body with a $C_R/D = 1.75$, with the exception of the fin with

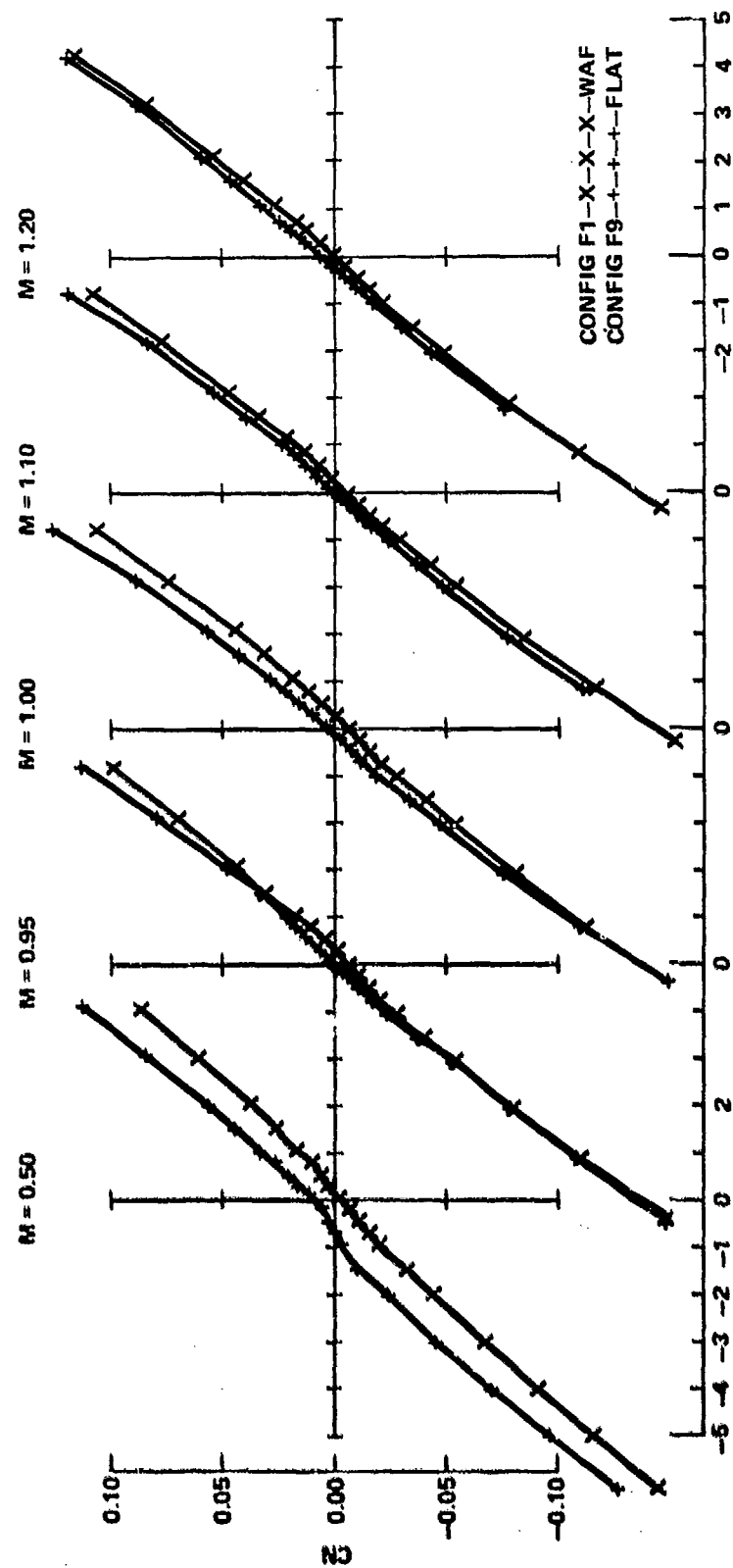


Figure 10. Comparison of WAF and flat fin normal force coefficient on reflection plane.

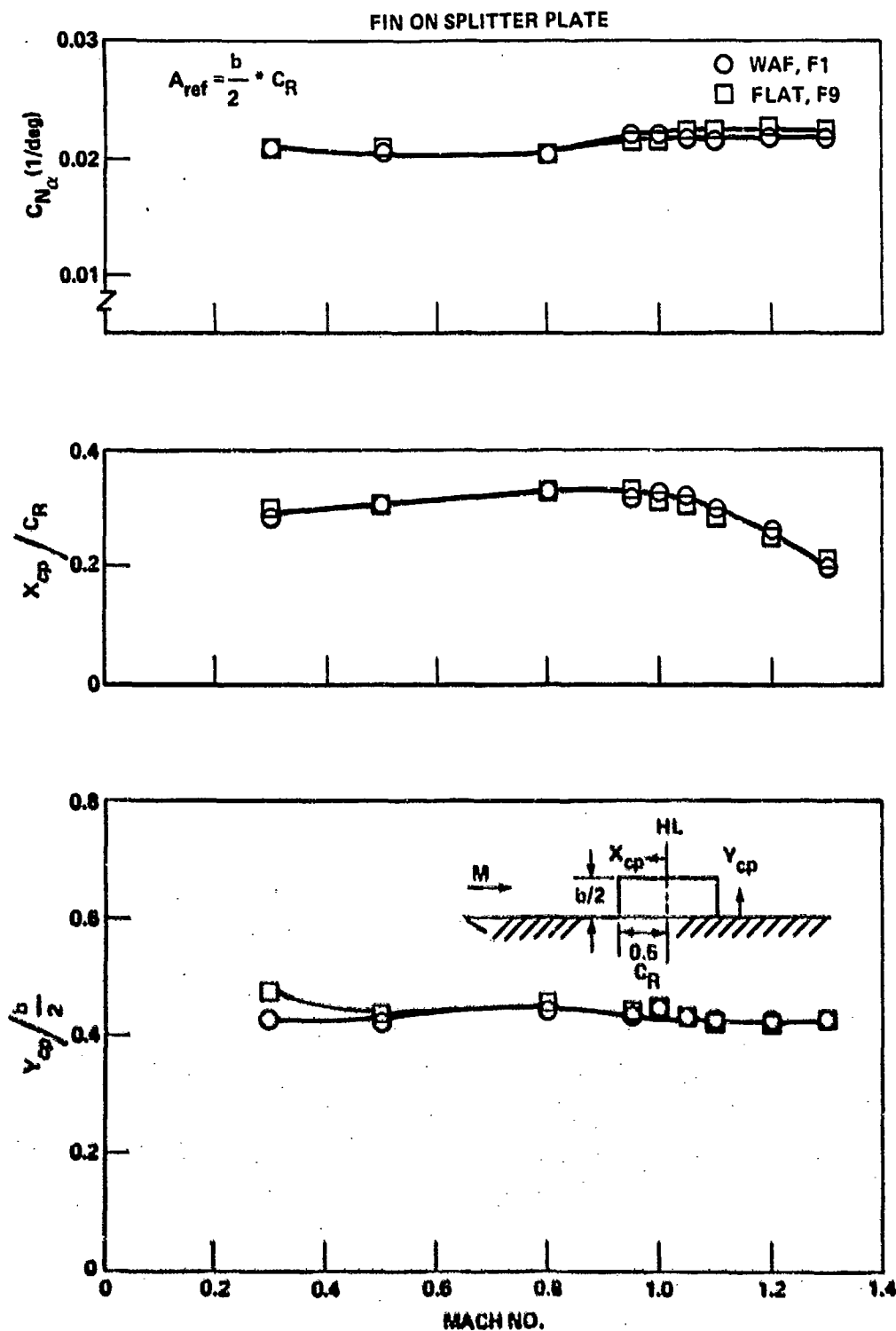


Figure 11. Comparison of WAF fin panel to flat fin panel static stability.

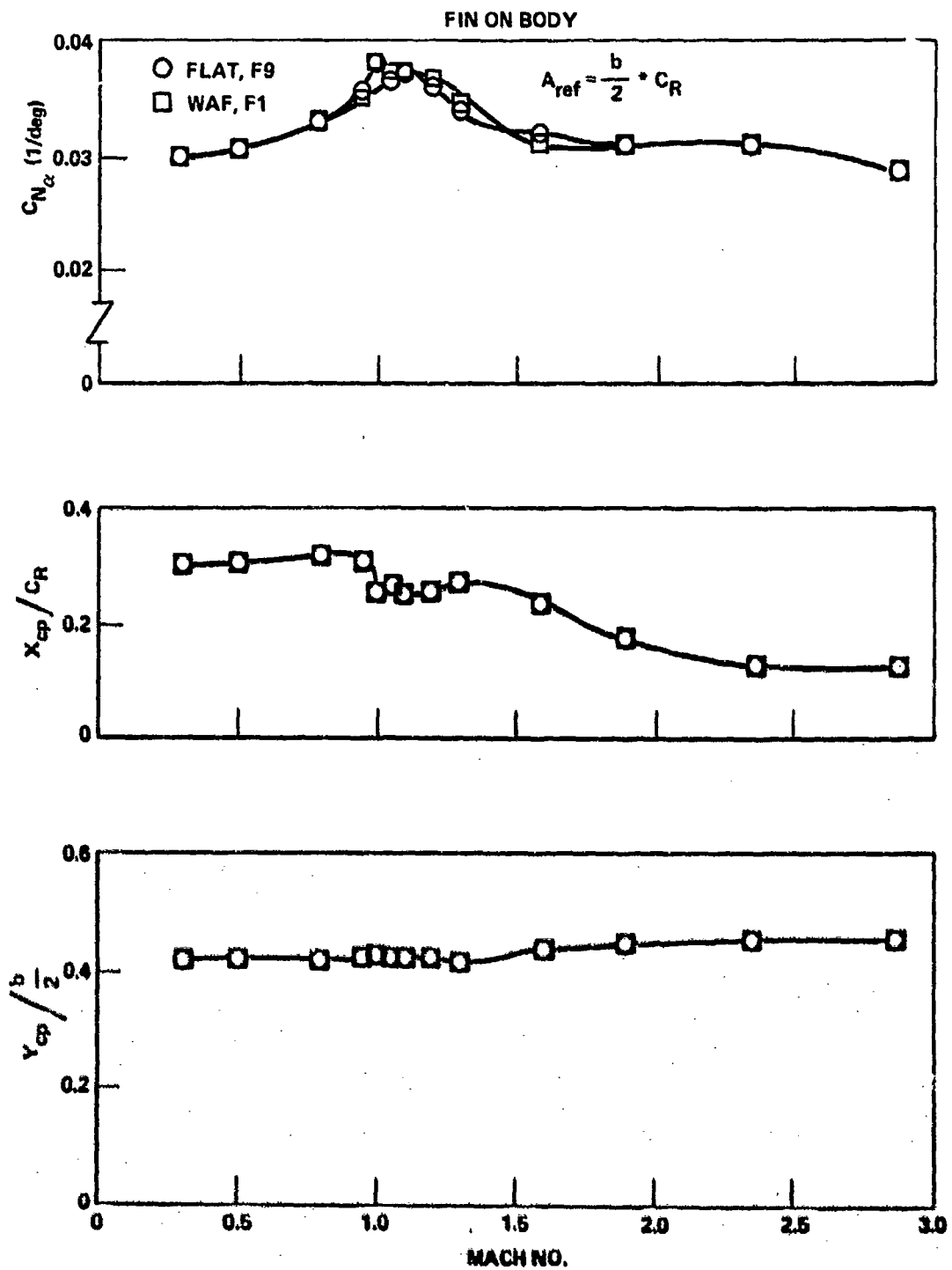


Figure 11. Concluded.

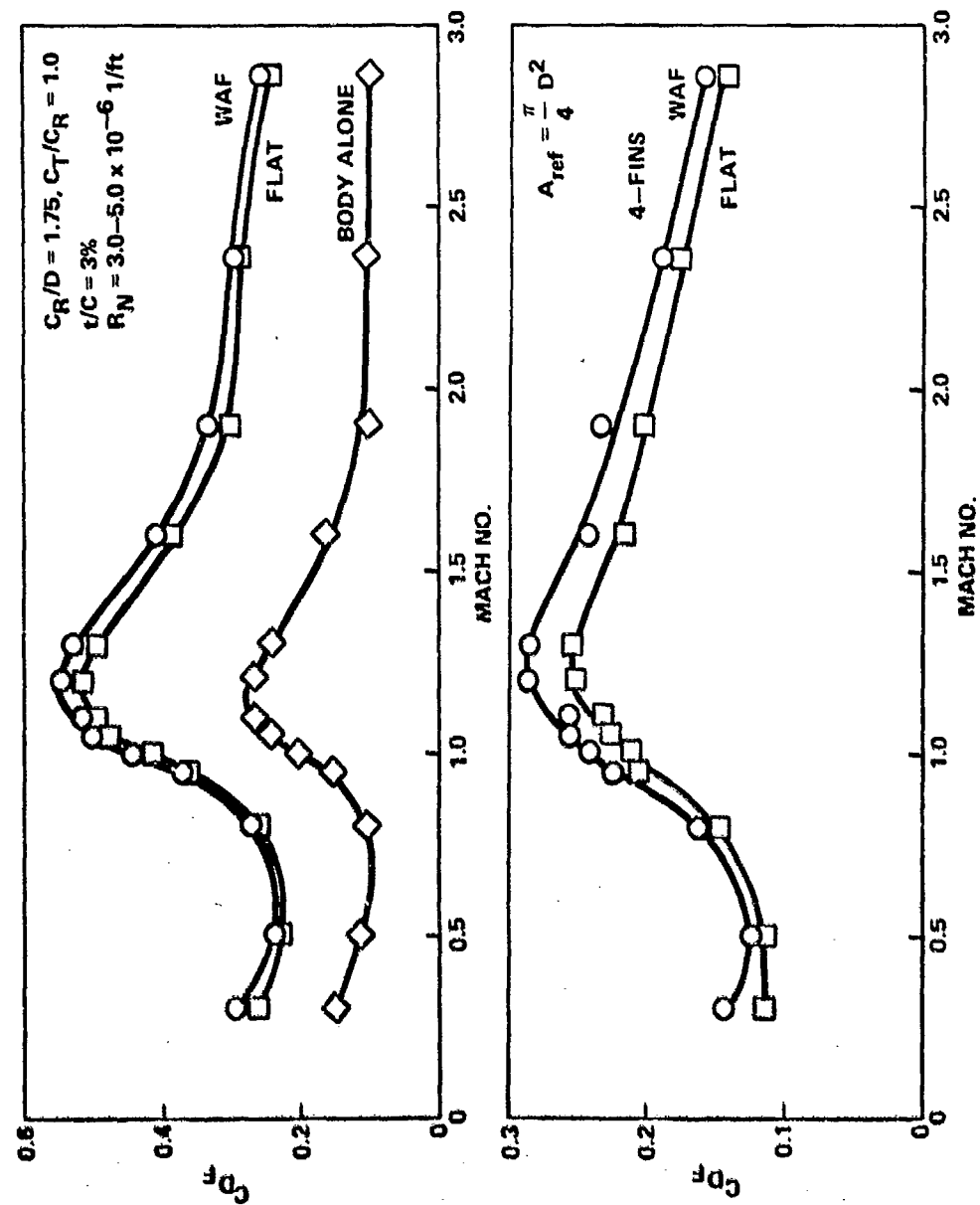


Figure 12. Comparison of flat and WAF drag coefficient at zero angle of attack.

maximum thickness $t/C = 0.045$ F8. This trend exists for fins with rectangular and trapezoidal planforms, for leading edge profile modification, and for modifications to the root chord (gap fin) and the tip chord. All roll moment coefficients are referenced to the area of body cross section $\pi D^2/4$, and reference length is the body diameter D . It is difficult to isolate and illustrate many specific parametric effects without pointing out the influence of another parameter. There is also the case of the influence of Reynolds number which, at this time, is not clearly shown to be an important parameter with the exception of the otherwise unexplained difference between the crossover point shown by the JPL free flight data and the results from static test. Grit was used as boundary layer trips on the body of JPL models, but grit was not used on fin leading edges which Mr. Jaffe (JPL) and this author agree may have been a mistake. The effect of three parameters are shown on Figure 13 for the standard TTCP WAF. The Reynolds numbers vary from 7 to 40×10^6 based on body length for the static test and for the JPL models was 2.5×10^6 . As can be seen, the effect of R_N on smooth and step-down body, except for JPL, shows differences well within data accuracy. Illustrated on this same curve is the variation of rolling moment with Mach number and the difference of trends with a smooth body and a step-down body which may more realistically simulate flight hardware hinge recesses. More information will be presented for the Mach number and body with step-down later in this report.

Other parameters which appear to have lesser influence on the WAF rolling moment are leading edge sweep and fin thickness (Figures 14 and 15). The surprising result from the leading edge sweep data is the level of magnitude, and the trend with Mach number appears very much the same as the rectangular fin with the same root chord length. Sweep of the leading edge did not show a shift in crossover Mach number as anticipated. The effect of modifying the leading edge shape is shown in Figure 16. There is a large change in roll moment, as expected, with the unsymmetrical leading edge. This may be related to regimes of subsonic and supersonic leading edge due to detached and attached shocks over the curved fin, which is neither an axisymmetric body of revolution or a two-dimensional surface. The symmetrical leading edge variation with included angles of 20.0° , 45.0° , and blunt show an effect transonically, but at supersonic speeds is incomplete at this time. Navy WAF pressure data [1] have shown the leading edge pressure difference between the convex and concave side to be larger than any other chordwise location, except $M = 1.3$ data which show the largest difference to occur at approximately 31% chord from leading edge. Unfortunately, neither the 20° or blunt leading angles have been tested supersonically. However, as presented by Featherstone [10], this leading edge pressure effect may be an inlet phenomenon due primarily to fin curvature and not influenced significantly by leading edge shape or fin thickness. Figure 17 presents the rolling moment coefficient for three rectangular planform WAF's with different chord length, therefore, having different

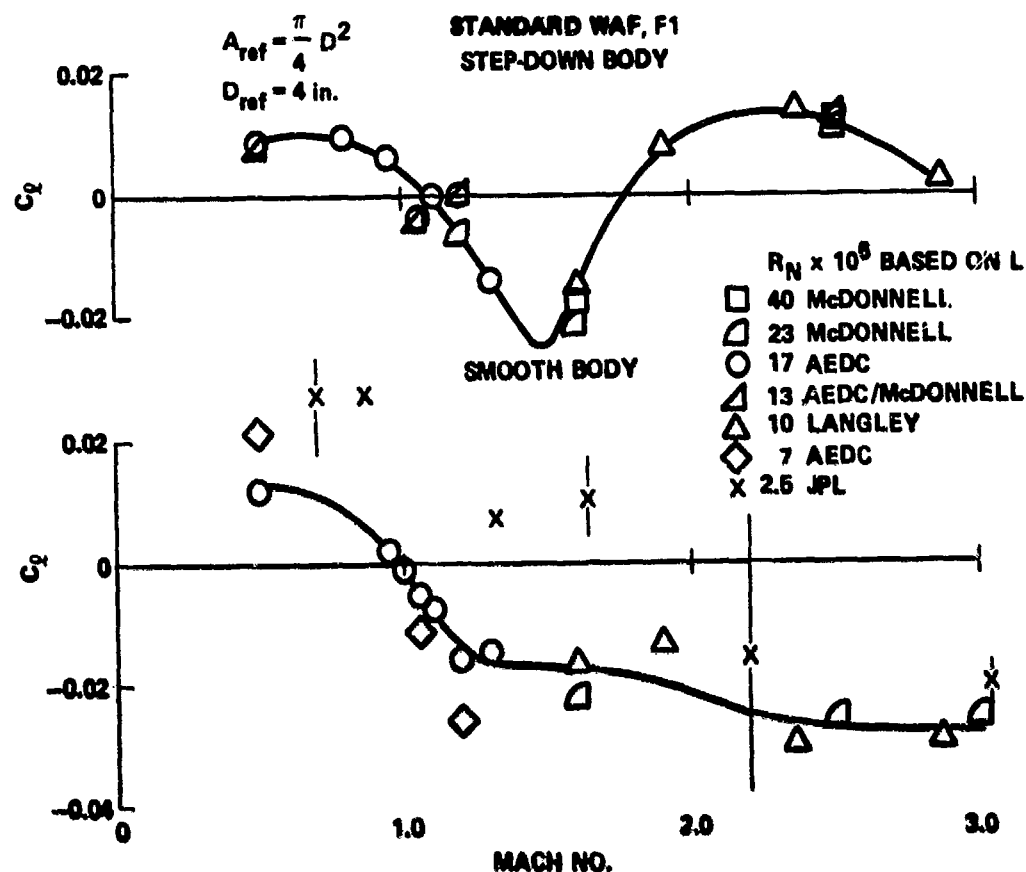


Figure 13. Effect of Reynolds number on zero angle of attack rolling moment coefficient.

aspect ratios. The primary influence seems to be the fin body juncture geometry and/or boundary layer, which in this case is fin root chord length rather than aspect ratio. Aspect ratio was also varied by sweeping the leading edge. The leading edge was swept up to 60° for $C_R/D = 1.75$, and a delta planform for $C_R/D = 1.0$. From these variations it is shown (Figure 15) that data with like root chord length tend to look similar and that the effect seen in Figure 17 may be a subsonic fin-body juncture (chord) length effect.

Additional modifications were made to the fin root and tip chord (F10 and F11, Figure 3 and Table 1). These were tested only at transonic speeds and show small effect on rolling moment coefficient (Figure 18).

One of the most significant changes in WAF rolling moment coefficient occurs with variation of angle of attack. The roll producing force increases with angle of attack at all Mach numbers and missile roll orientation and is directed toward the fin away from the fin center of curvature. Figure 19 presents the WAF compared to the flat fin at supersonic Mach numbers from the Langley and McDonnell tests [7,8].

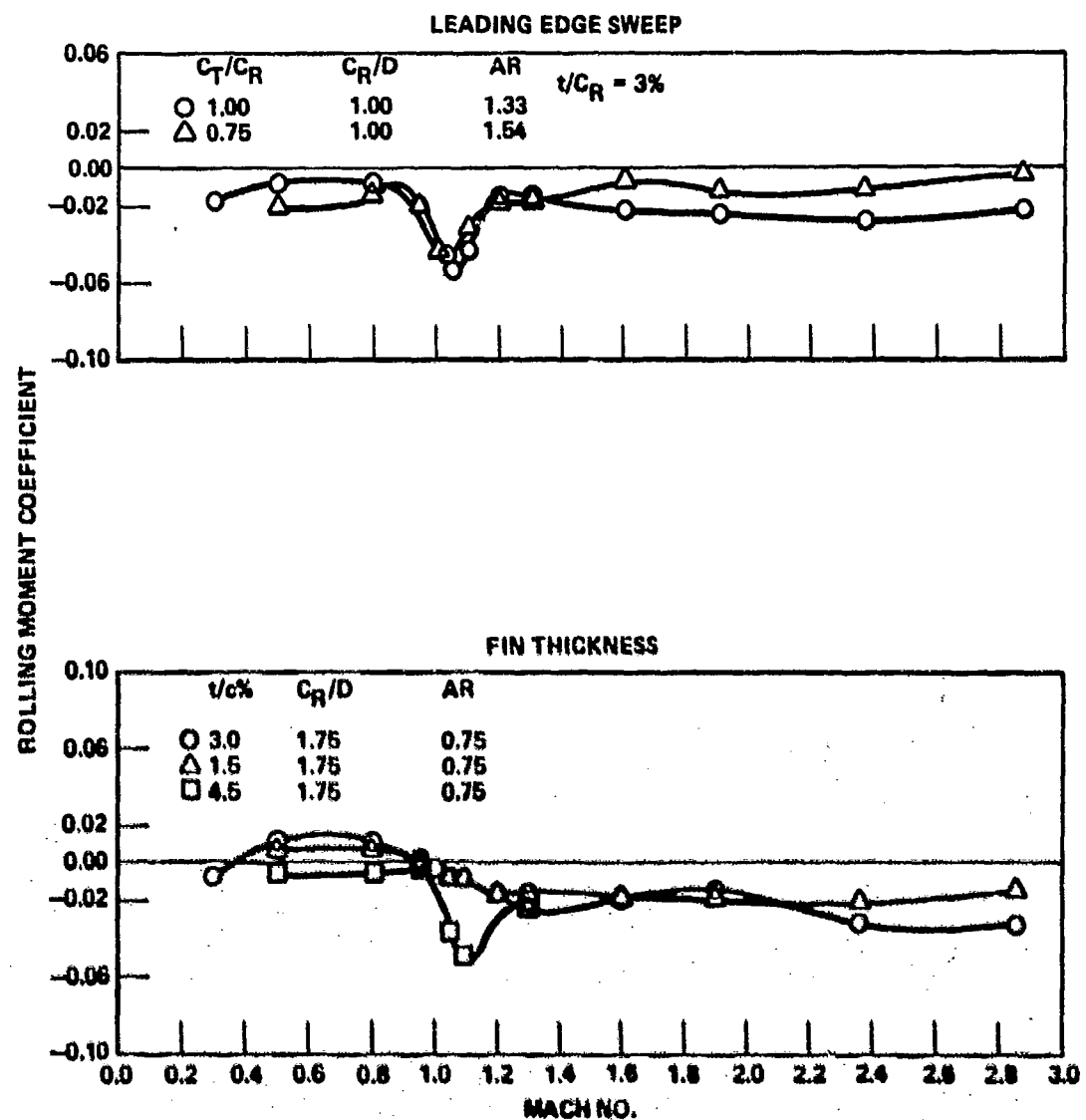


Figure 14. Effect of fin leading edge sweep and fin thickness on WAF rolling moment coefficient, $\alpha = 0$.

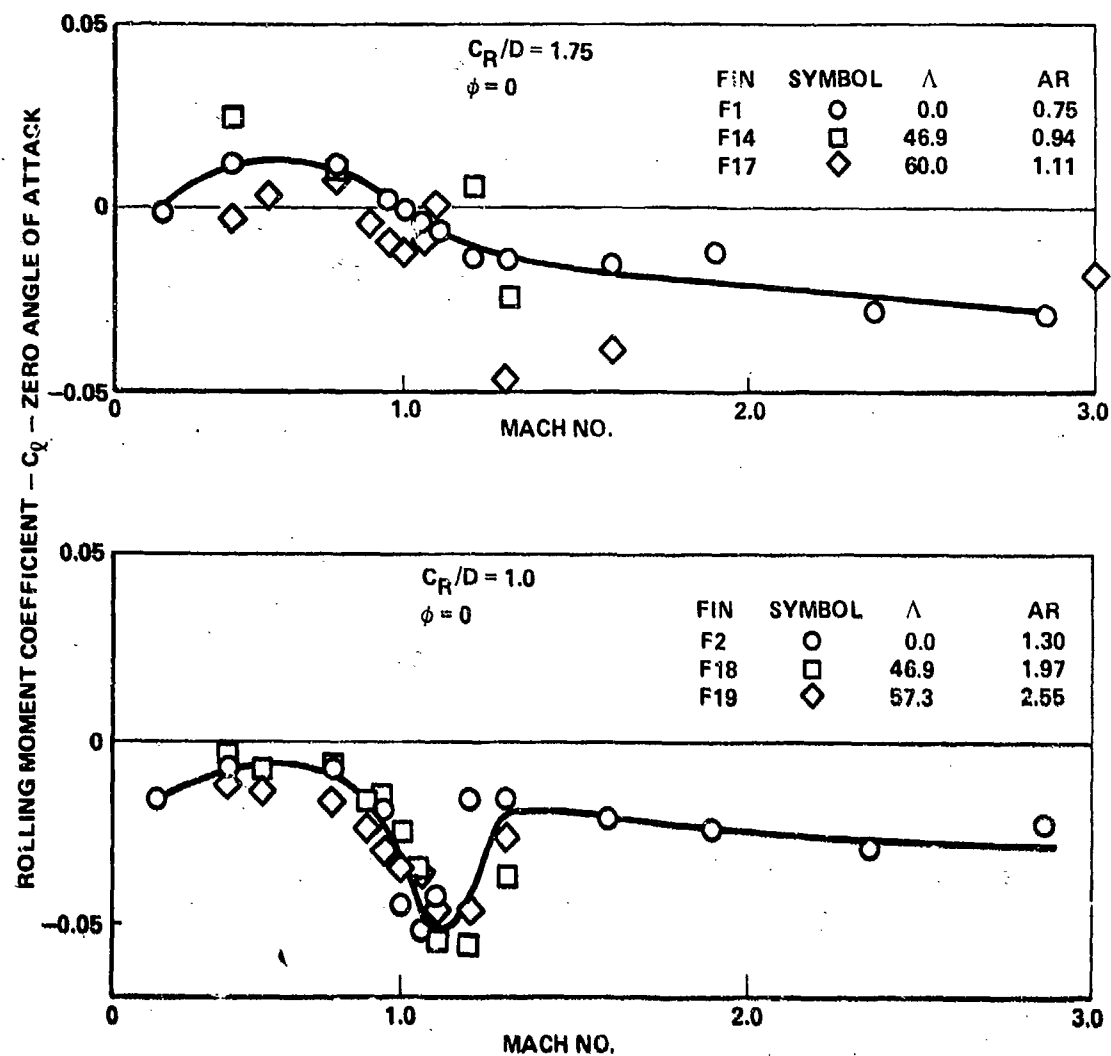


Figure 15. Effect of fin leading edge sweep and aspect ratio on rolling moment coefficient.

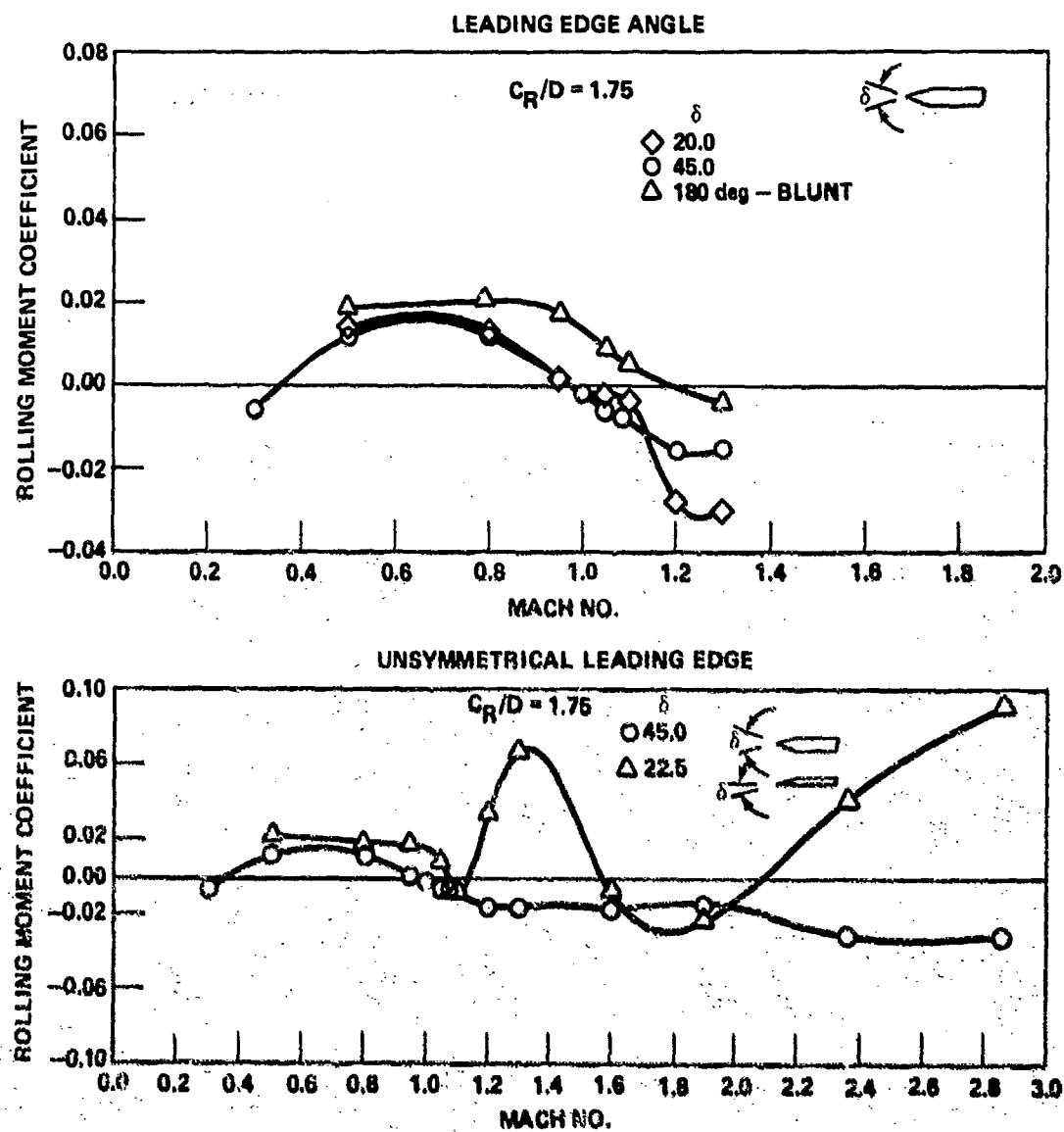


Figure 16. Effect of leading edge shape on WAF rolling moment, $\alpha = 0$, $t/C_R = 3\%$.

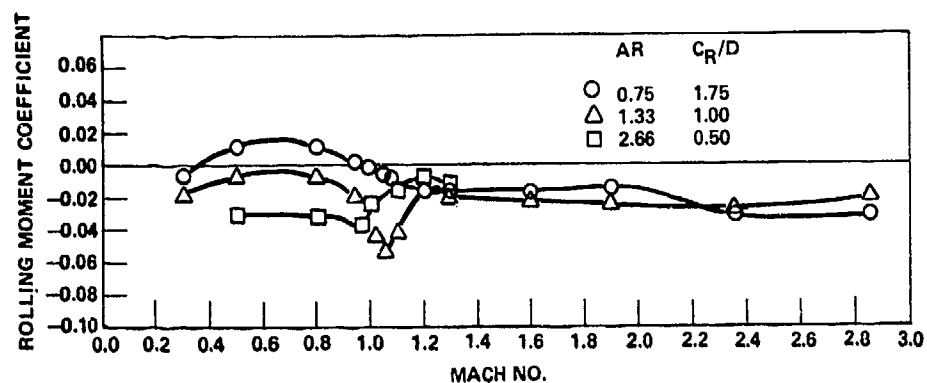


Figure 17. WAF rolling moment coefficient versus Mach No., $\alpha = 0$, $t/C_R = 3\%$.

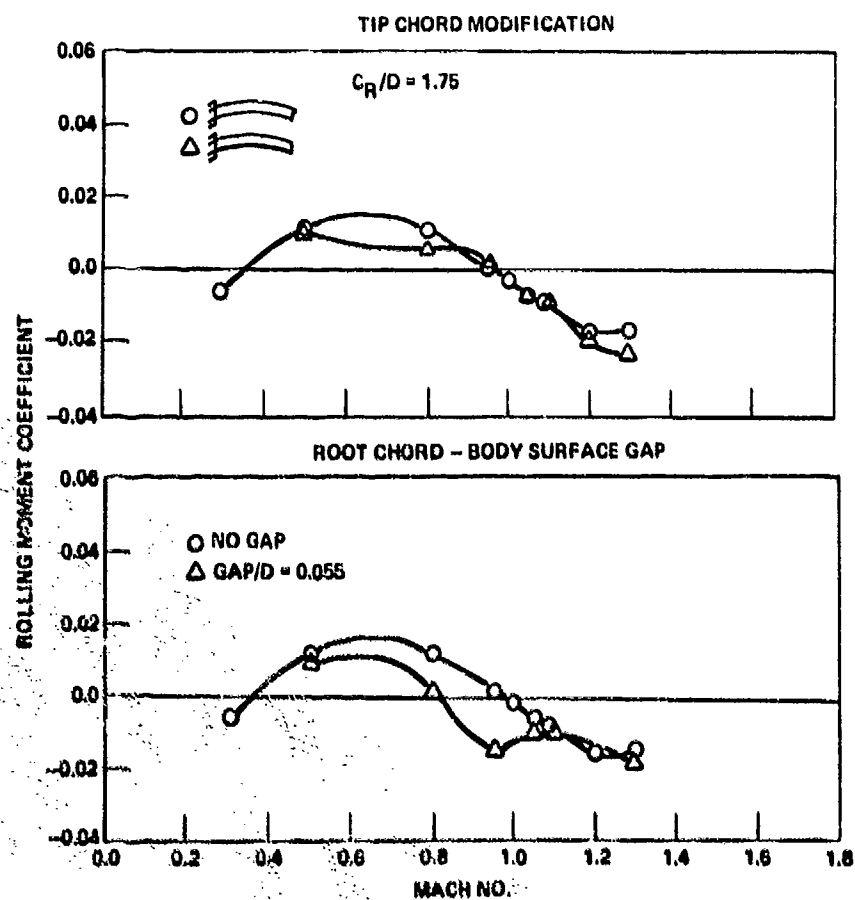


Figure 18. Effect of modifying WAF root and tip chord cross section on rolling moment, $\alpha = 0$, $t/C = 3$ percent.

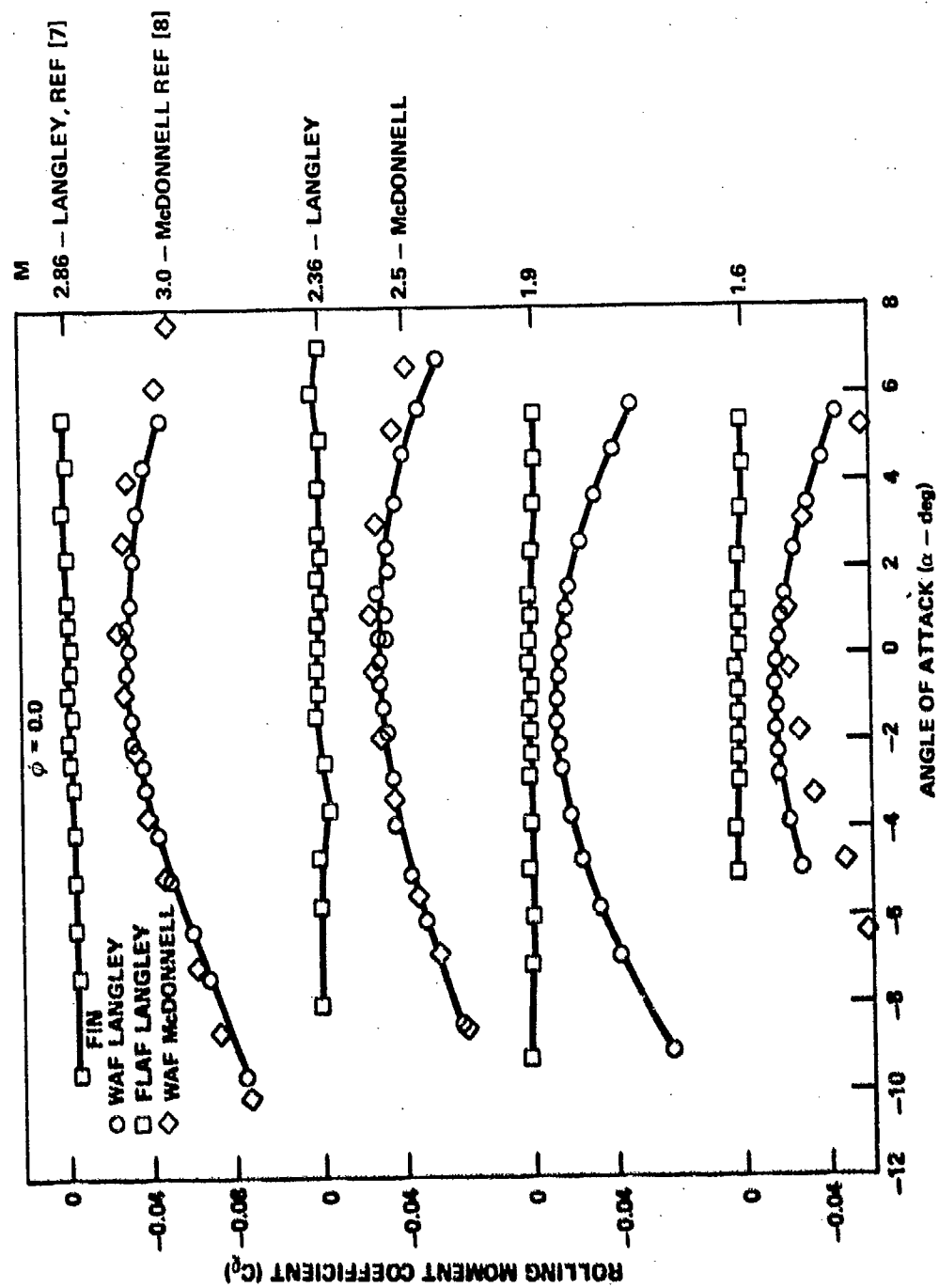


Figure 19. Comparison of flat and WAF rolling moment coefficient versus angle of attack and Mach No.

This trend was shown to be essentially unchanged with missile roll attitude with fins of equal exposed span and to a lesser extent at subsonic Mach numbers [2,3,8]. The rolling moment coefficients throughout the Mach number range tested are shown with varying angles of attack for fins F1 and F2 on Figures 20 and 21. Navy ZUNI data have also demonstrated this phenomenon and it has been shown by Stevens [12] that this driving moment may be a useful design tool for avoiding roll-yaw resonance problems during missile flight.

The span for all but two WAF's tested had nearly equal exposed semispans of 0.66 body diameters. These two (F20 and F21) had reduced spans of 0.54 and 0.35, respectively. The zero angle of attack rolling moments are shown at supersonic Mach numbers (Figure 22). Significant reductions in induced rolling moments occur at Mach numbers above two for WAF's with spans less than a quarter circle. This suggests the possibility of tailoring the induced rolling moment variation with Mach number by varying the fin radius of curvature. This design procedure is only allowed when adequate space exists around the rocket for the fin curvature to depart from the body surface. The variation with angle of attack and missile roll attitude are shown in Figures 23 and 24 for the three spans. There are two significant effects that should be noted. There appears to be much less variation with angle of attack induced with shorter span WAF (Figure 23); however, at the supersonic Mach numbers, roll moment will be dominated by body vortex and span (Figure 24). The interaction is not necessarily unique to the WAF but is related to the relative position of the body vortex core at angle of attack, fin span, and missile roll attitude, where the fin arrangement is not symmetrical at angle of attack (e.g., $\phi = 22.5^\circ$).

The step-down body effect is probably the most significant trend that must be considered in WAF designs requiring a hinge recess and/or body step-down geometry. The standard WAF is shown on the smooth and step-down body in Figure 15. All symmetrical leading edge fins on the smooth body show only one crossover point for Mach numbers less than 3.0, but the step-down body demonstrated an additional crossover at low supersonic Mach numbers and is opposite to the Featherstone postulation that the force at supersonic Mach numbers is directed away from the WAF center of curvature. Two additional fins that show this are shown in Figure 25. These fins have a 1-caliber root chord; one is rectangular and the other has a 20.6° swept leading edge. Comparisons of rolling moment coefficient between the smooth and step-down body for four fin planforms are shown on Figures 26 and 27. The flow mechanism that causes this trend may be the key toward development of supersonic analytical methods.

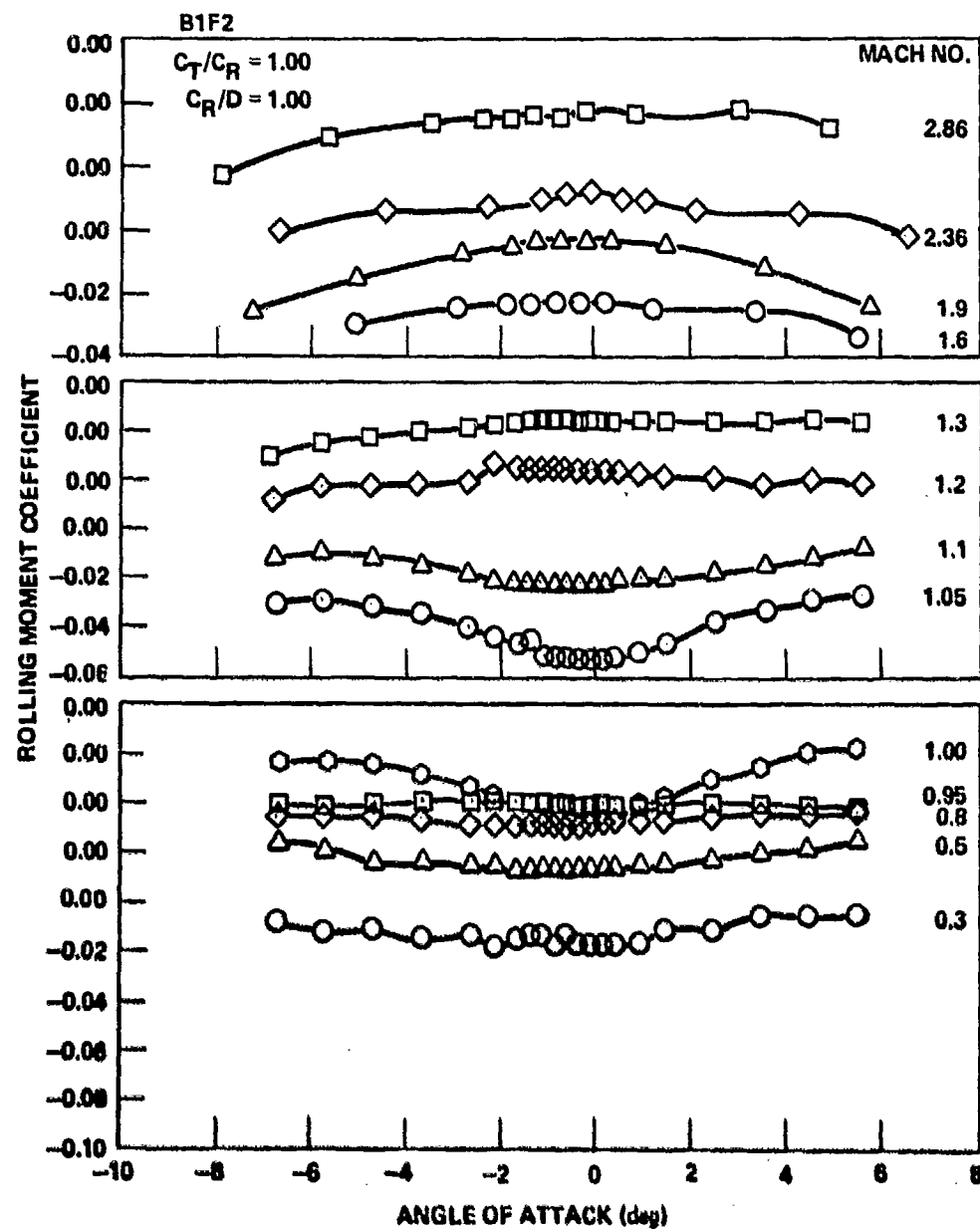


Figure 21. Variation of WAF rolling moment coefficient with angle of attack, $AR = 1.33$.

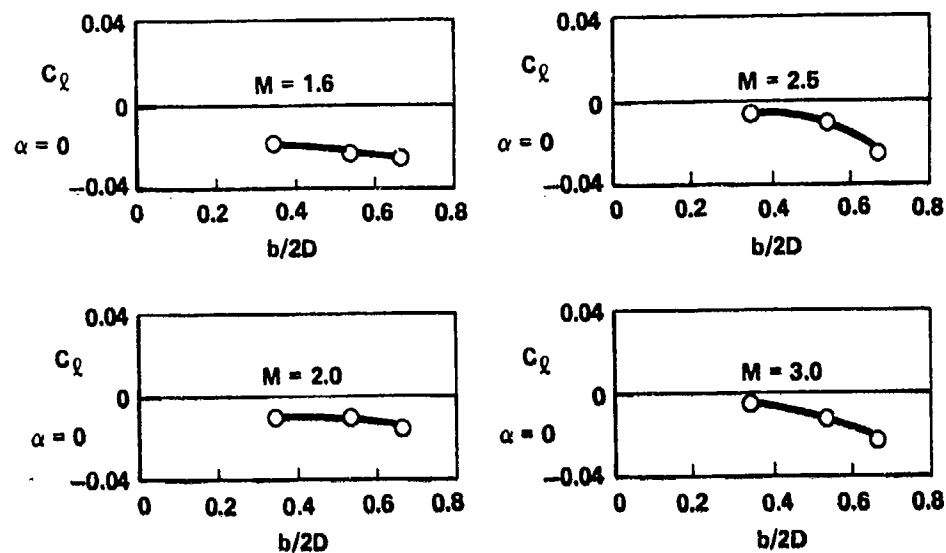


Figure 22. Effects of span on WAF induced rolling moment
 $C_R/D = 1.75$.

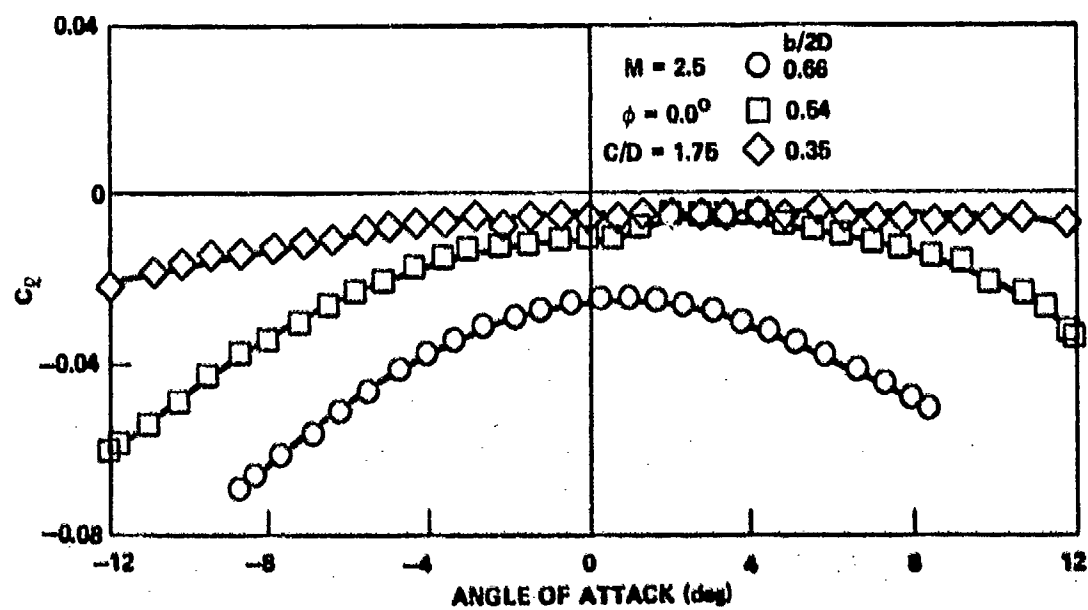


Figure 23. Effect of fin span and angle of attack on WAF
 rolling moment coefficient.

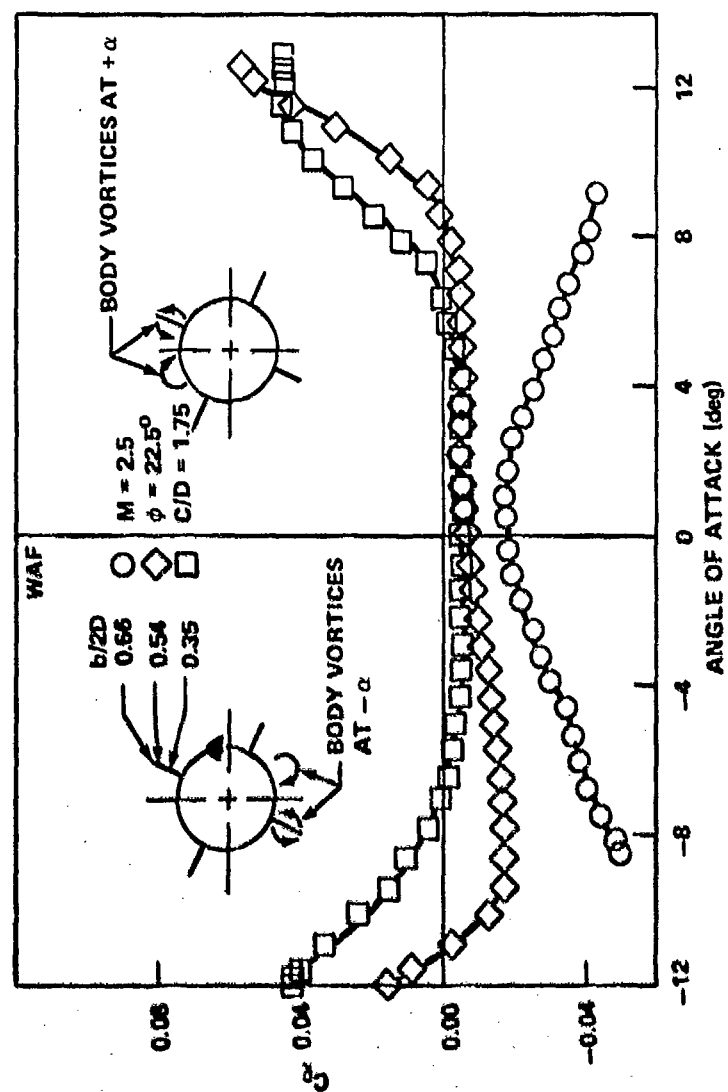


Figure 24. Effect of body vortex at angle of attack on WAF rolling moment.

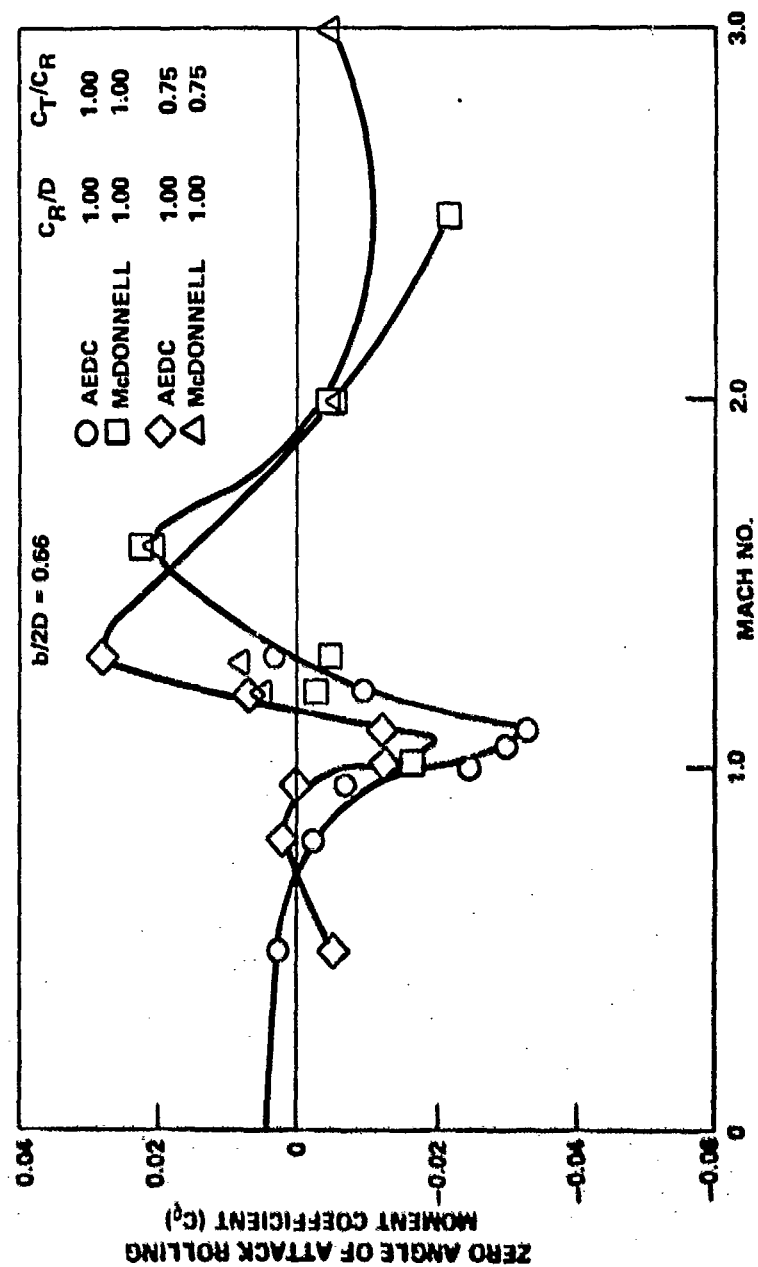


Figure 25. Effect of leading edge sweep and step-down body on roll moment coefficient versus Mach No.

EFFECT OF STEPDOWN BODY ON WAF ROLLING MOMENT
COEFFICIENT, $\alpha = 0$, $t/C_R = 3$ PERCENT, $C_R/D = 1.75$

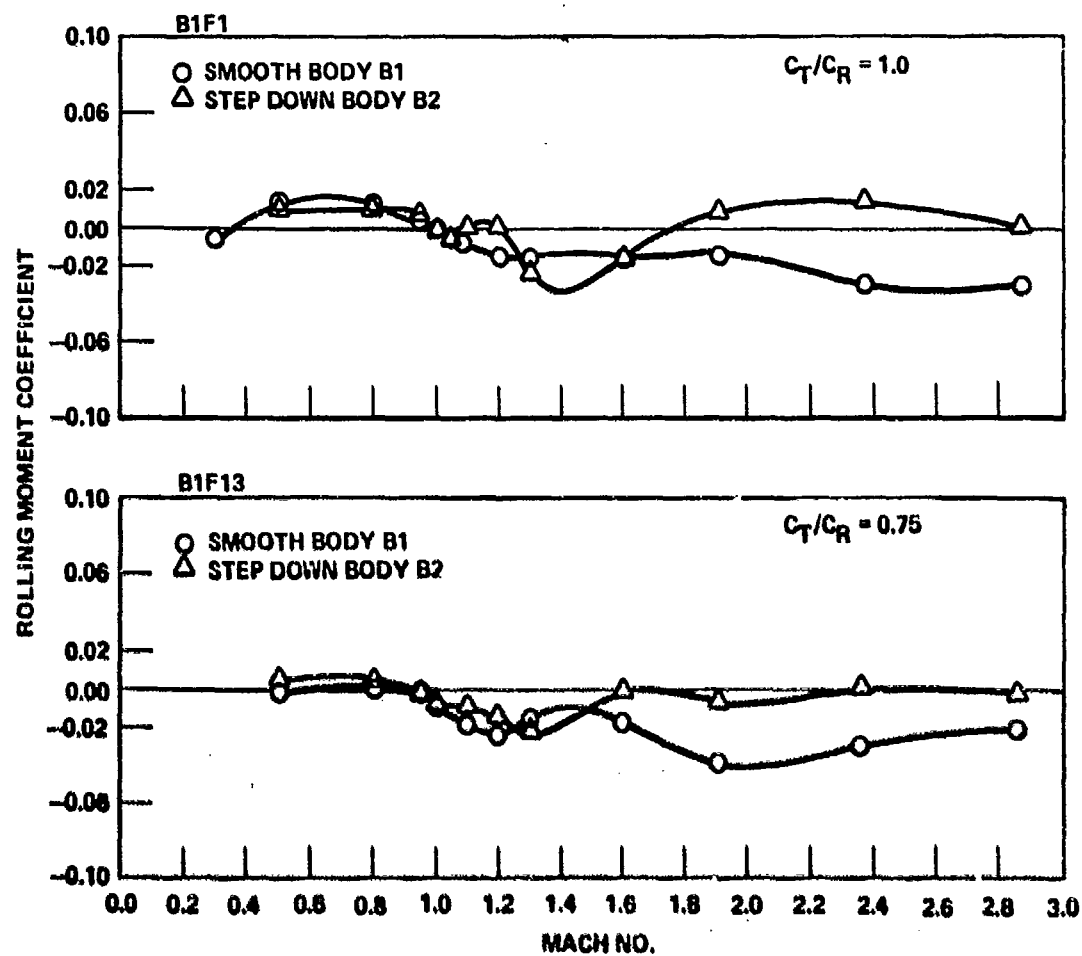


Figure 26. Effect of afterbody shape on WAF rolling moment.

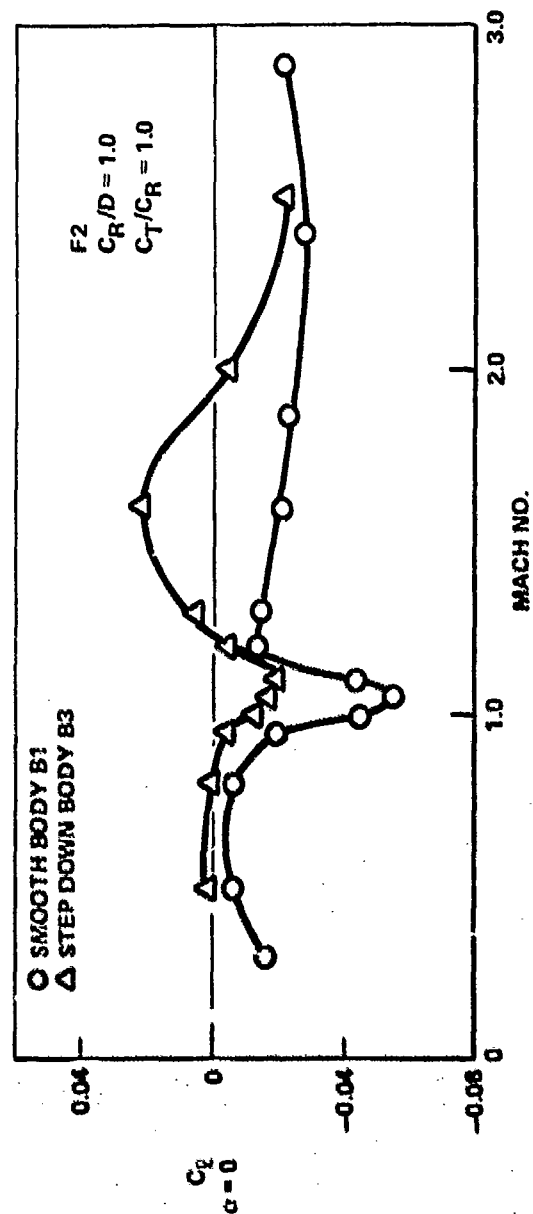
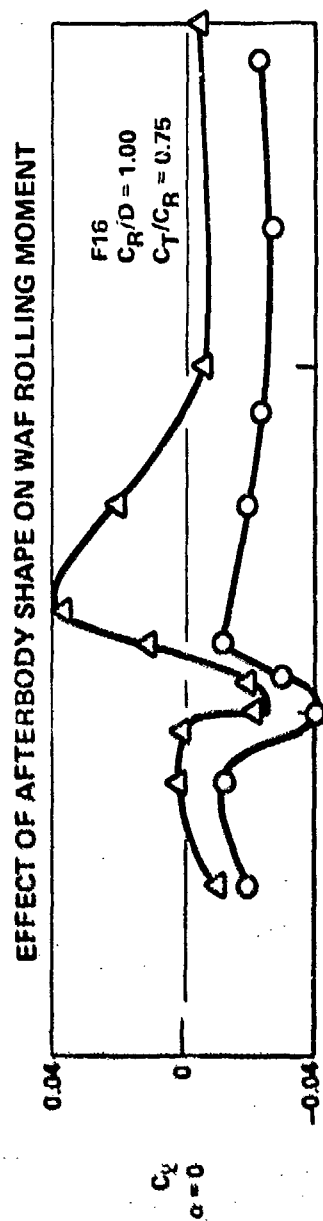


Figure 27. Comparison of WAF and flat fin side force coefficient.

VI. SIDE FORCES AND MOMENTS

It has been suggested [11] that in addition to induced rolling moments, the WAF causes side force and moment variations with pitch angle of attack. A typical comparison between flat and WAF at supersonic Mach numbers is shown as a function of angle of attack in Figure 28. Nothing was observed during this series of testing (Figures 29, 30, and 31) that substantiates the generation of cross derivatives of significant magnitude over the angle of attack range $\pm 6^\circ$, contributable to cruciform WAF at subsonic and transonic Mach numbers. Small variations with angle of attack may have been seen at supersonic Mach numbers as shown in Figure 28. ZUNI data at Mach 3.0 are shown to have a similar trend to the MICOM data at Mach 2.86. The step-down body does not show any significant differences in side force or moment with angle of attack variation.

The same mechanism that causes large roll moment changes with short span fins at roll orientation and angle of attack (Figure 24) also induces large yawing moments (Figure 32). This trend is not considered to be unique to the WAF and may be, as expected, a function of roll orientation especially for angles of attack (at supersonic Mach numbers) where body vortex cores rise to the fin tip. Missile roll rate will tend to average out this phenomenon and usually will not present a problem in flight. Outside of this effect, cruciform WAF's do not appear to have significant cross derivatives except possibly at Mach numbers above 2.5. Geometric arrangements of the WAF other than cruciform can be expected to induce side force/yawing moment variations with angle of attack and roll attitude. These would include: three-fin configurations; staggered longitudinal configurations; WAF with alternate opening directions; and opening angles other than the fully open as defined in this report.

VII. OPENING ANGLE

The standard WAF was tested on the smooth body for seven opening/closing angles defined as fully open when a line passes the body center, the fin pivot point, and tip chord. The fin is fully closed and conforms to the body surface at $\theta = 135^\circ$. The test matrix is shown in Table 3. Most transonic data were obtained at AEDC [3], and all supersonic data were obtained at McDonnell Douglas Aerophysics Laboratory [8]. Figure 33 shows the model with three opening angles of 0, 45, and 90°. Fin lift effectiveness (Figure 34) is shown for three Mach numbers over the range of closing angles tested. Lift effectiveness is defined as the ratio of the fin normal force at a given closing angle θ to the fin normal force at the fully open case $\theta = 0.0$. The fin center of pressure appears to be essentially invariant with closing angle and is a function only of Mach number as for the fully open case. A geometric fit of $\cos^2 \theta$ is shown in comparison to the fin lift effectiveness. Figure 35 shows the zero angle of attack rolling moment variation with

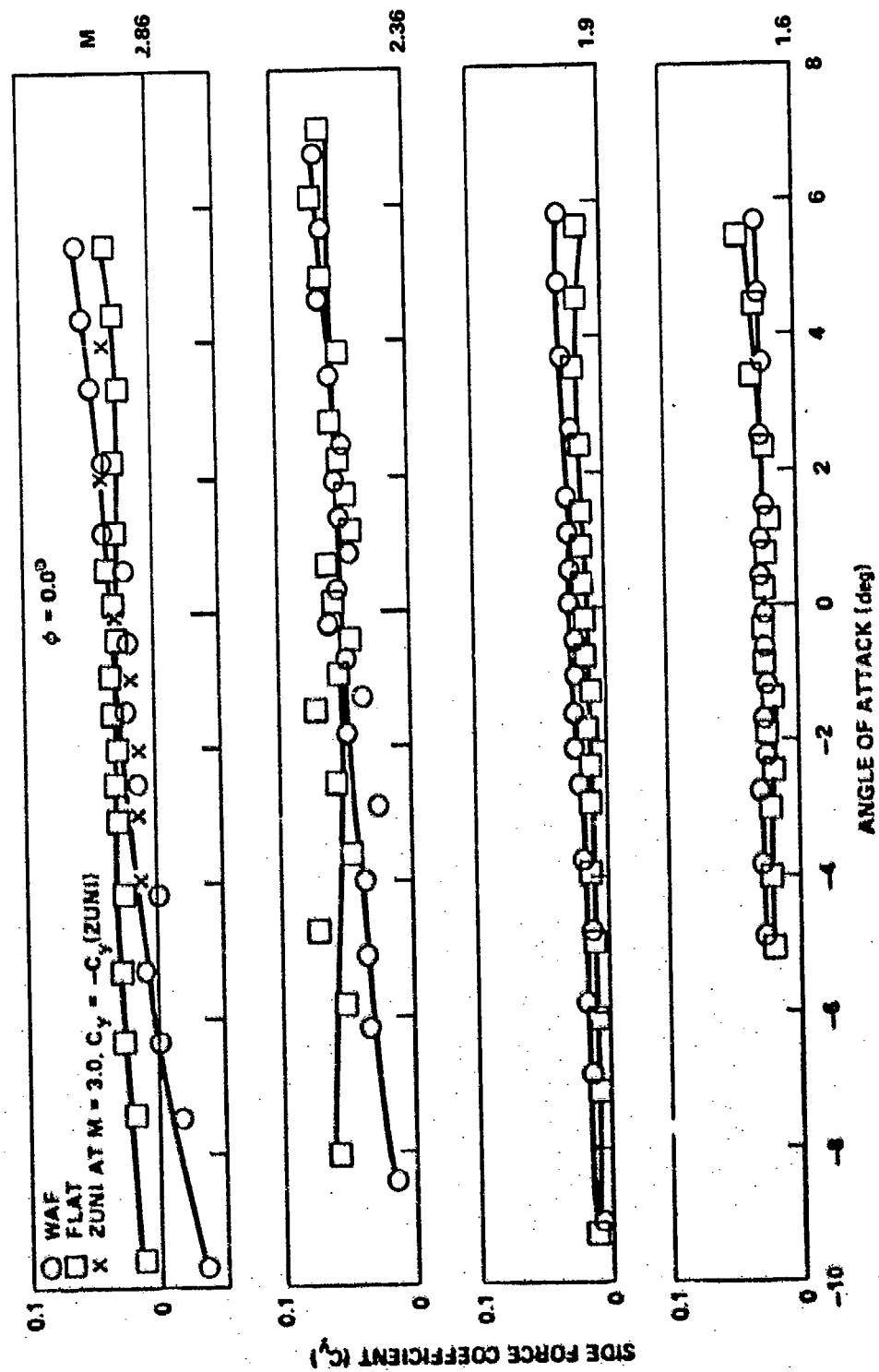


Figure 28. Comparison of WAF and flat fin side force coefficients.

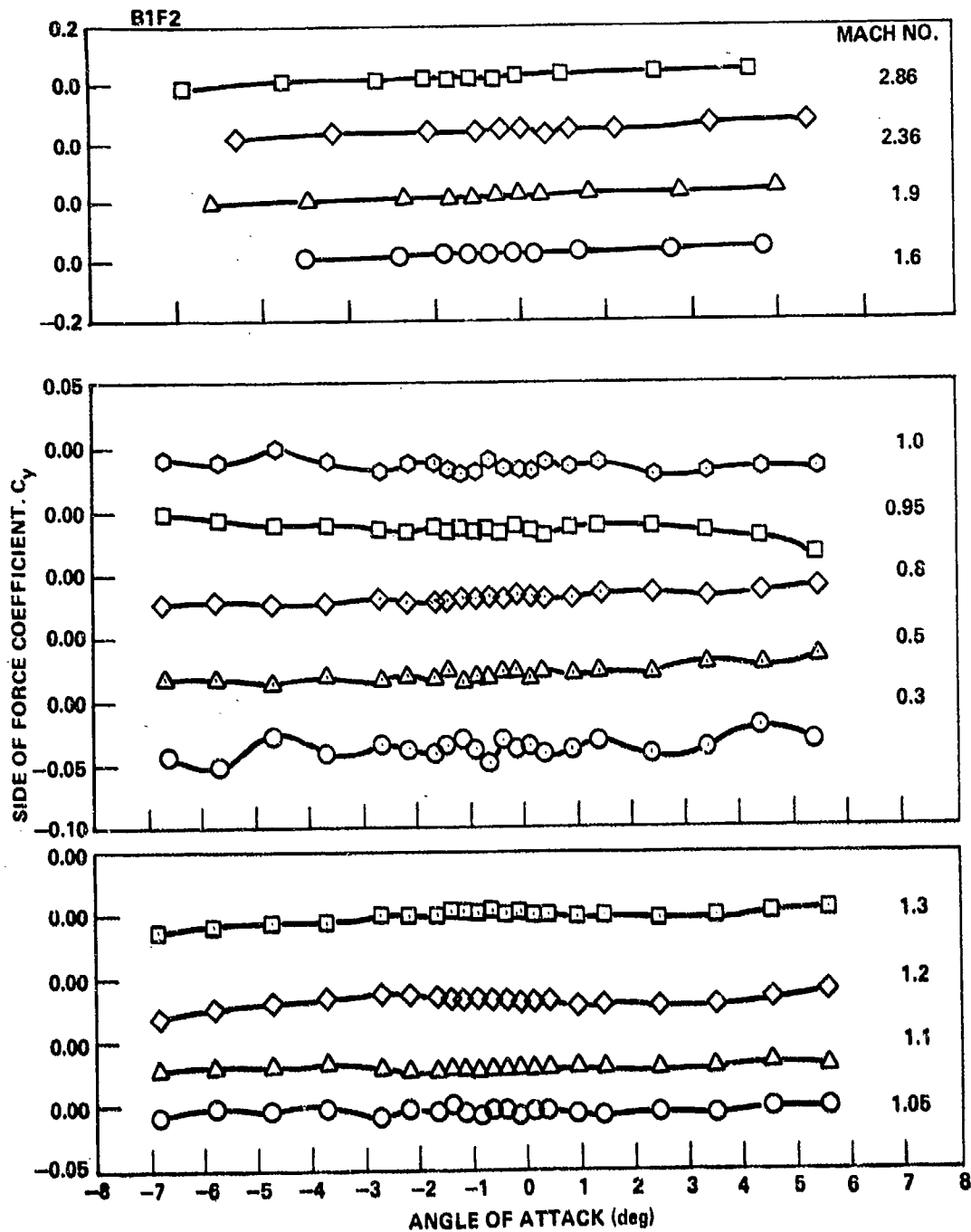


Figure 29. Variation of side force coefficient with angle of attack, WAF, $AR = 1.33$, $C_R/D = 1.00$, $C_T/C_R = 1.00$, $\phi = 0$.

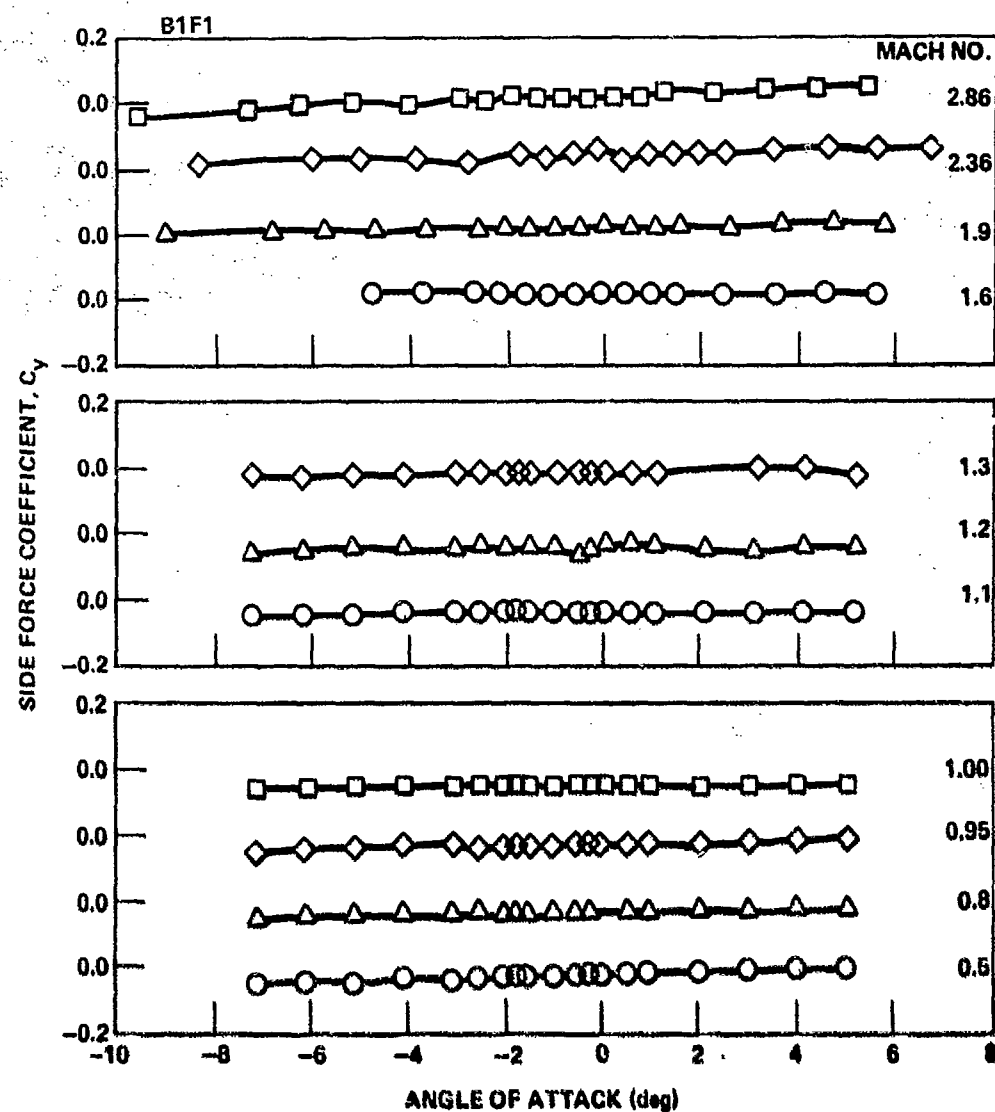


Figure 30. Variation of side force coefficient with angle of attack, WAF, $AR = 0.75$, $C_T/C_R = 1.00$, $C_R/D = 1.75$, $\phi = 0$.

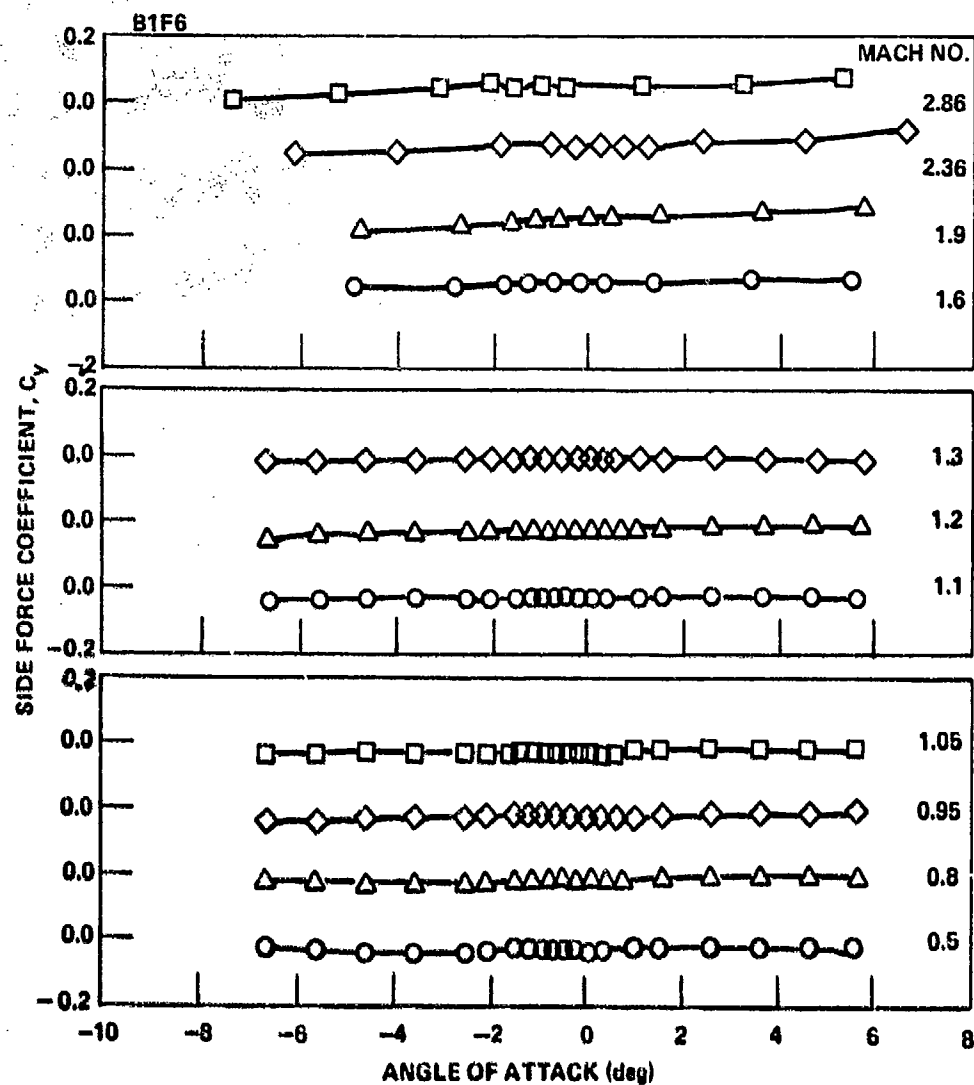


Figure 31. Variation of side force coefficient with angle of attack, WAF, $AR = 0.75$, $C_R/D = 1.0$, $C_T/C_R = 1.0$, unsymmetrical leading edge, $\phi = 0$.

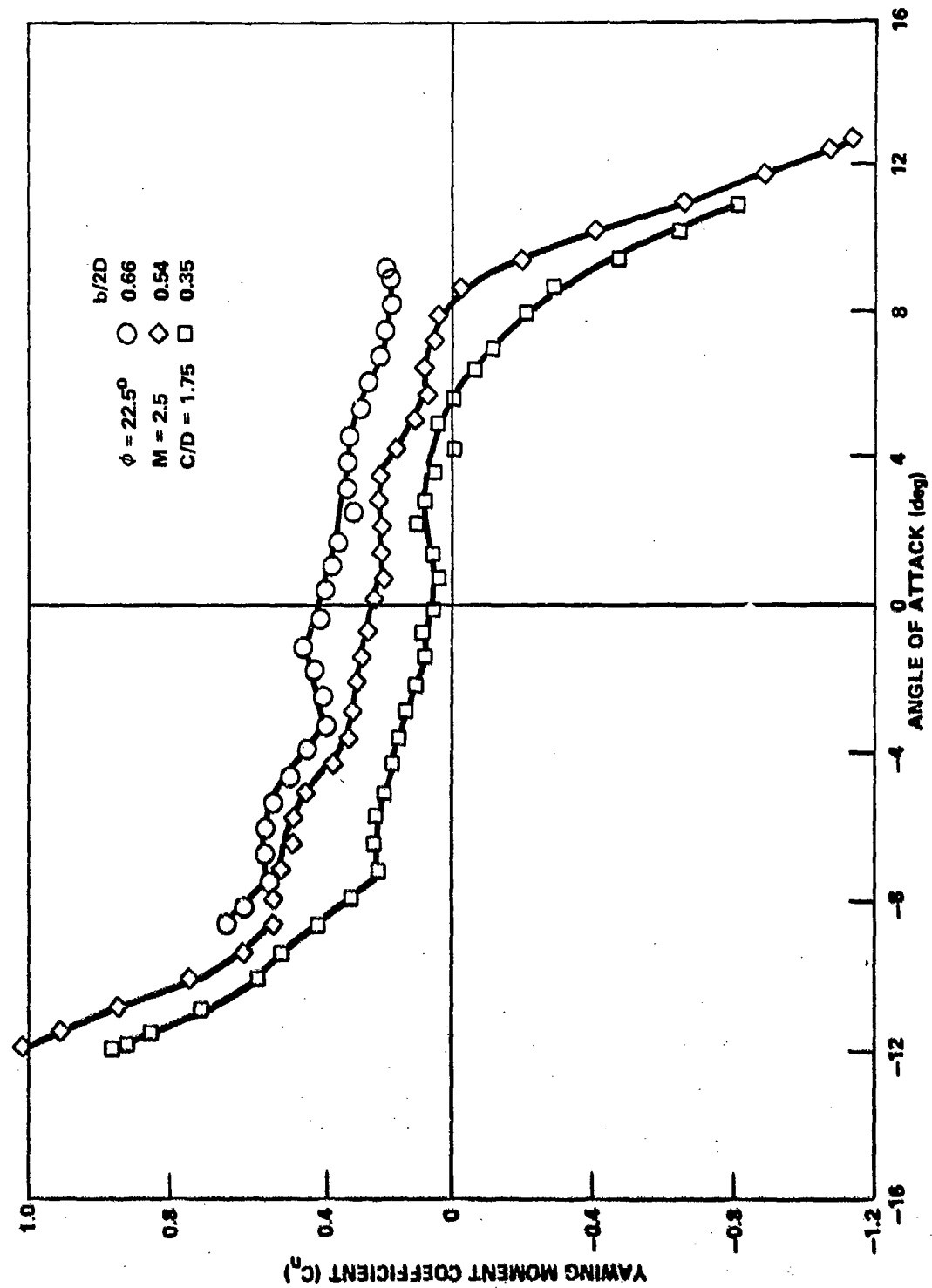




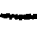









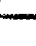


















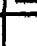


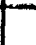









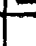












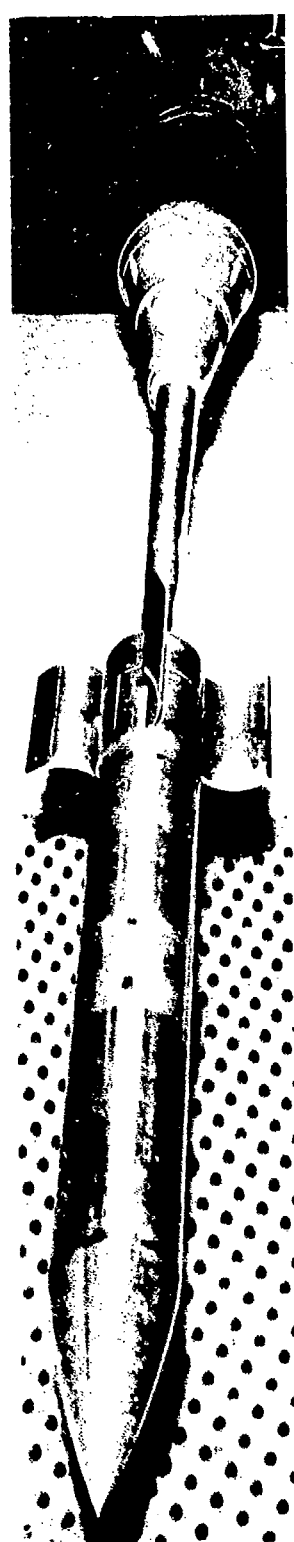


Figure 32. Effect of body vortex at angle of attack on yawing moment.

TABLE 3. SUMMARY OF WAF OPENING ANGLE TEST

OPENING <	MACH NO.													
	0.5	0.6	0.8	0.9	0.95	1.00	1.05	1.10	1.20	1.30	1.60	2.00	2.50	3.00
-10.0														
10.0														
22.5														
45.0														
90.0														
112.5														

 - SOLID SYMBOLS: 0, 22.5, 45, 67.5° ROLL ANGLE
 - SOLID SYMBOLS: 0, 22.5, 45° ROLL ANGLE
 OPEN SYMBOLS: ZERO ROLL ANGLE ONLY



$\theta = 0$



$\theta = 45$



$\theta = 90$

Figure 33. WAF model with opening angle variation.

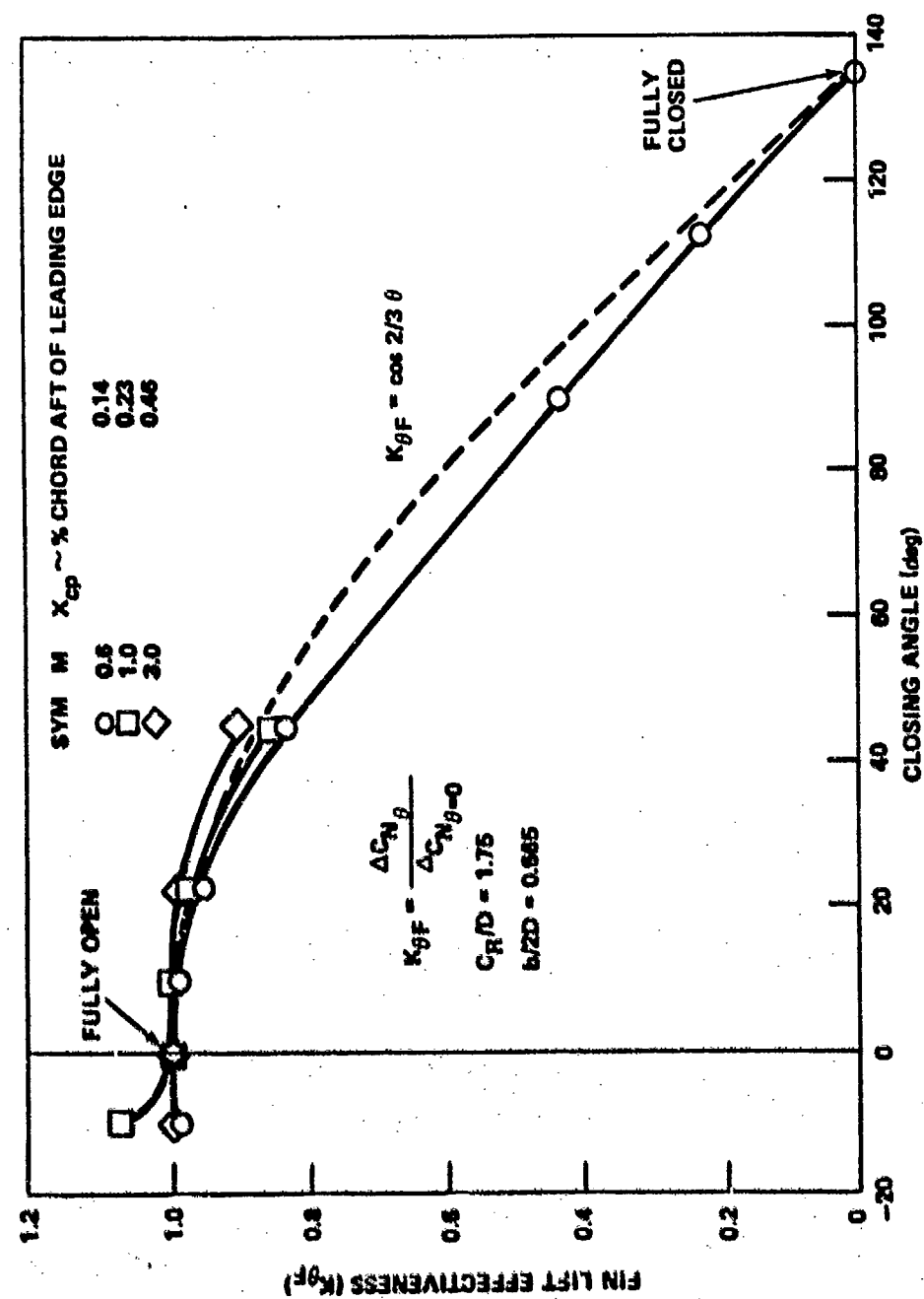


Figure 34. The ratio of fin lift effectiveness at closing angles.

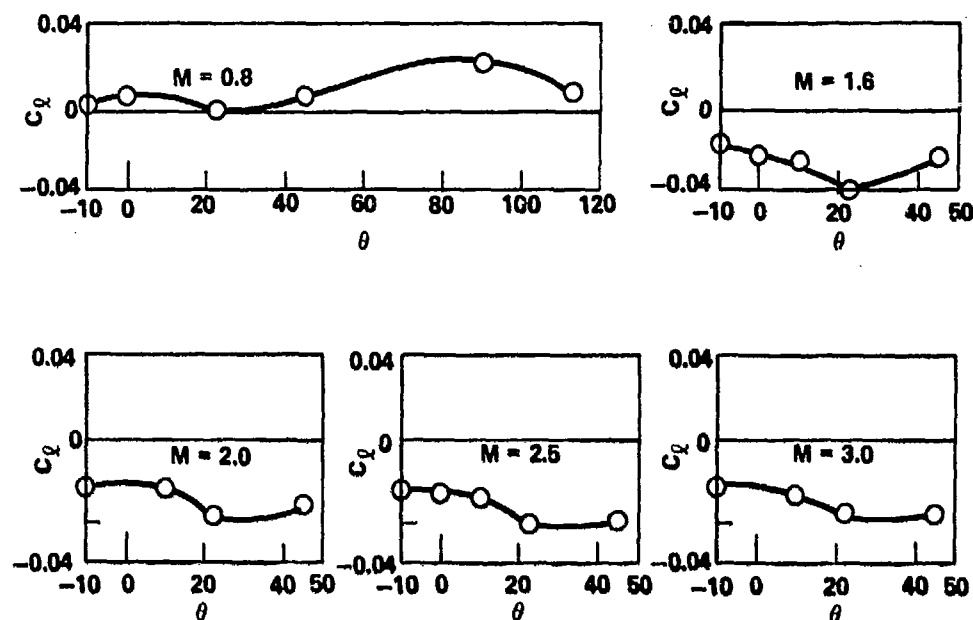


Figure 35. Effects of opening angle on WAF rolling moment zero angle of attack $C_R/D = 1.75$, $b/2D = 0.665$.

closing angle for Mach 0.8 to 3.0. No large influence was noted for small variations and, at any given angle, appear to follow the roll moment variation with Mach number as the fully open case does. At angles of attack above 6° some side force and yawing moment change was observed at opening angles other than zero.

VIII. WAF ROLL DYNAMICS

Tests were conducted where roll damping was measured for several fin configurations. Included in this was a comparison between a flat fin and the standard WAF. These data are in a MICOM report [9]. The model was spun up in the wind tunnel by an internal hydraulic motor. At a prescribed roll rate, the motor clutch was released and the model was allowed to free spin until the steady state roll rate was reached. Roll damping for one of the WAF's and one flat are shown to vary little (Figure 36). Theoretical calculations of $C_{\dot{\alpha}}$ by modified slender body

theory are shown to be good except at transonic speeds. Figure 37 shows the measured steady state roll rate for the WAF with fin cant angles of 0° and 1° at Mach numbers from 0.3 to 1.3. A comparison of the flat fin and WAF is shown for the 1° cant. The roll rate for the flat fin and WAF remains approximately the same through Mach number 0.8. Above Mach 0.8 the WAF deviated sharply away decreasing until at Mach 1.3 the roll rate was essentially zero. Thus the free spinning results substantiate the abrupt negative shift in rolling moment shown by the static

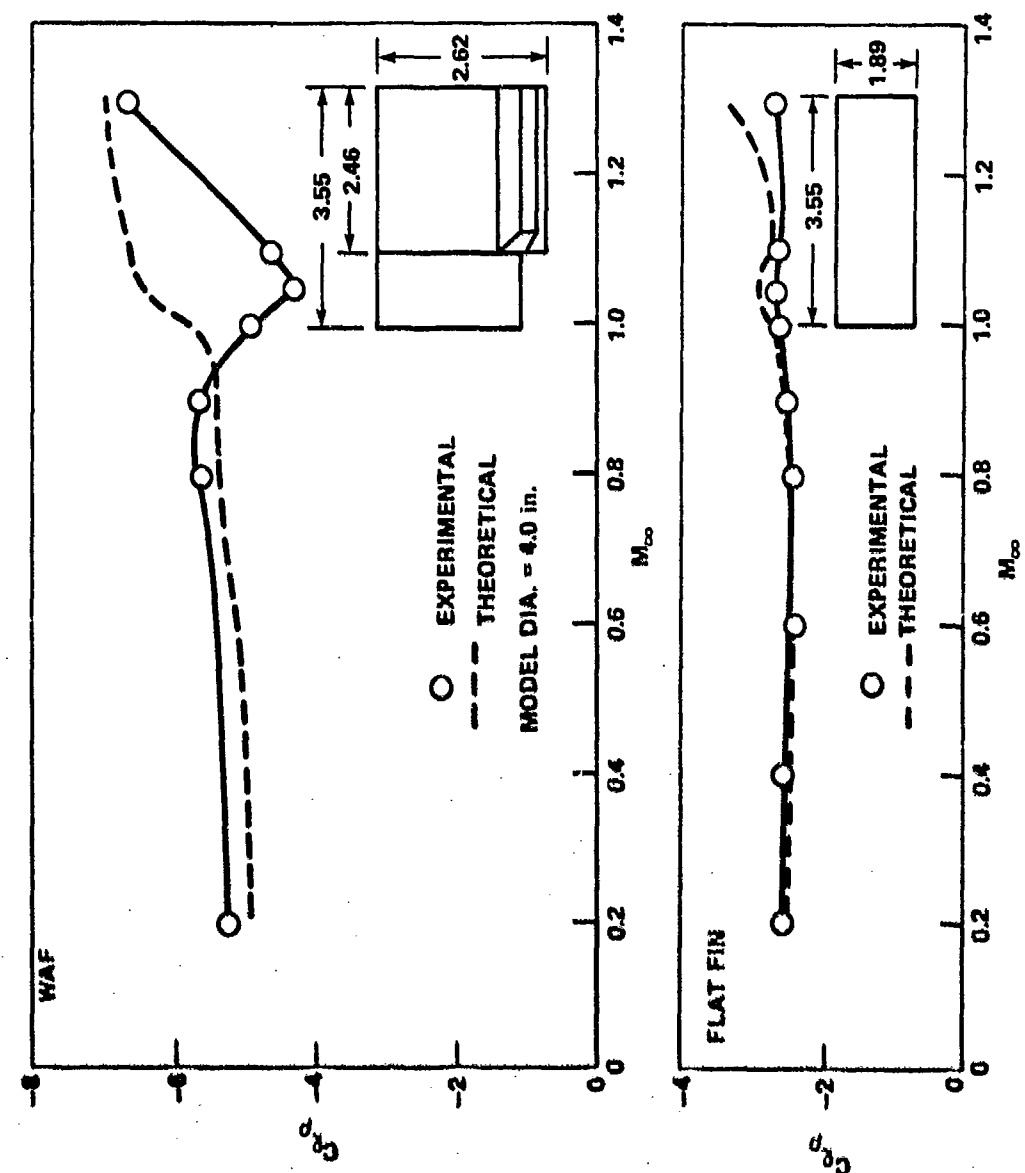


Figure 36. Comparison between theory and experiment.

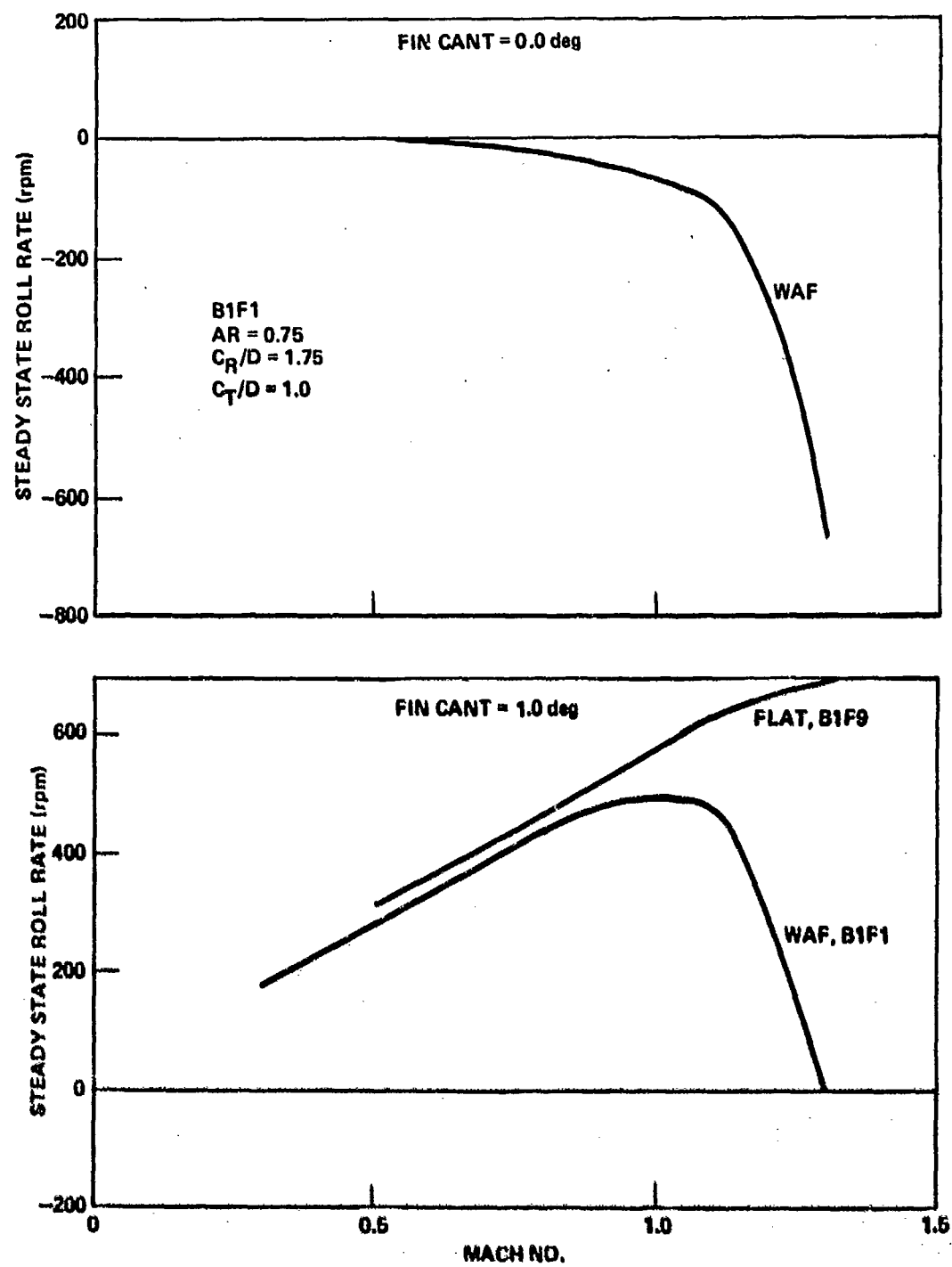


Figure 37. Experimental steady state roll rate of WAF and flat fin with fin cant.

data (Figure 13). The effect of fin cant (incidence) on WAF static rolling moment coefficient at zero angle of attack is shown through the transonic Mach numbers on Figure 38. These data are for the fin with geometry [9] shown in Figure 36, and the data implies that for moderate cant angles the self-induced WAF rolling moment simply produces a bias in total rolling moment. This is verified by the free spinning data shown in Figure 37.

A three phase investigation was conducted by JPL. Several small scale models were flown in the JPL 20-inch wind tunnel (Figure 4). Some were flown solely for obtaining rolling moment and roll damping coefficients, others were flown for a bi-planar dynamic investigation. A sting-mounted free spinning test was conducted initially to observe the roll direction of models with WAF as a function of Mach number. Data for the standard WAF and equivalent flat fin from the AEDC spinning test, theoretical estimate, and the JPL free-flight data for the flat and WAF are shown on Figure 39. The JPL data points (vertical lines indicate spread) have too much scatter for a thorough analysis. Even though some had initial roll rates with and against the fin fold direction, the scatter prohibits definition of roll damping for spin in any given direction.

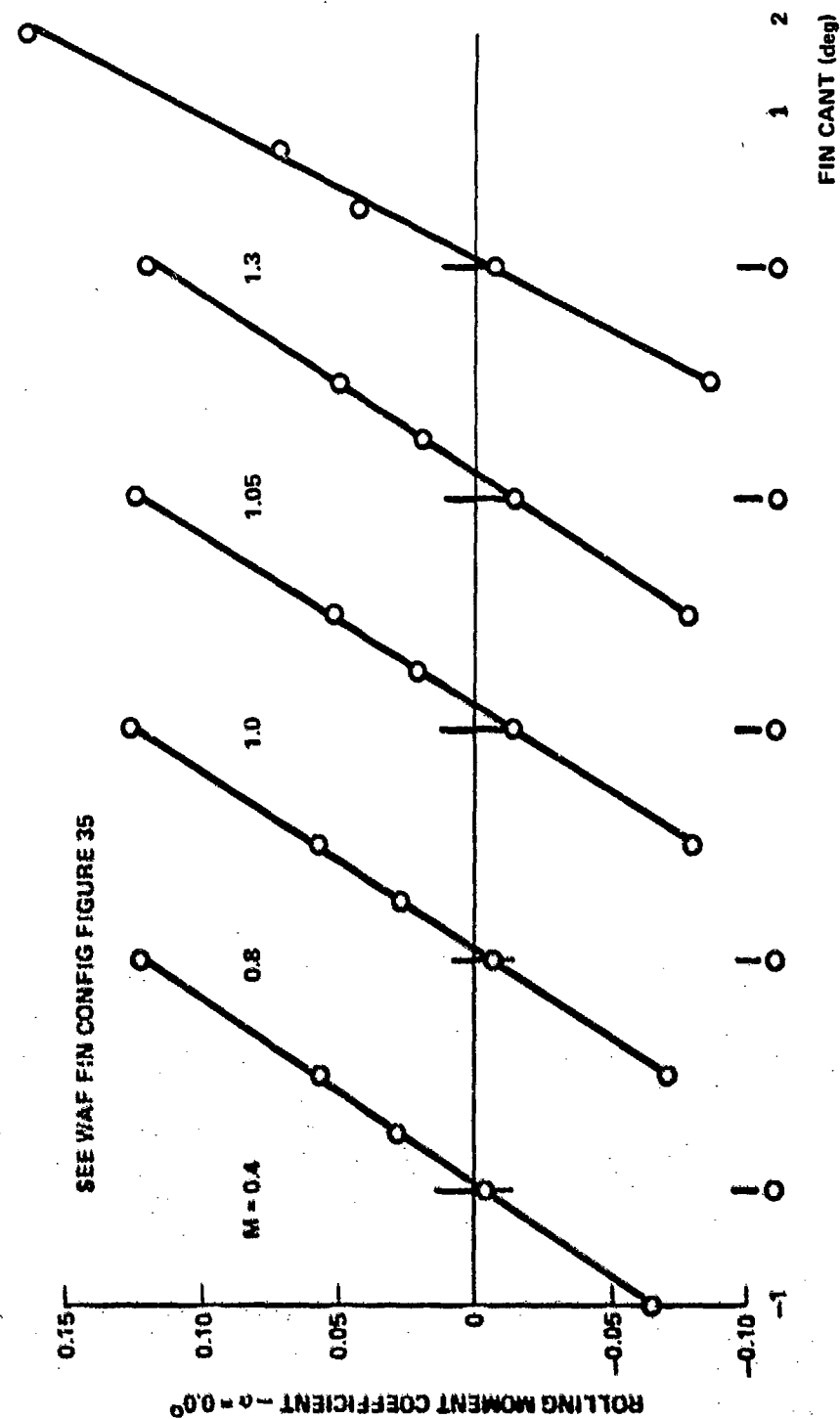


Figure 38. WAF rolling moment coefficient with varying incidence and Mach No.

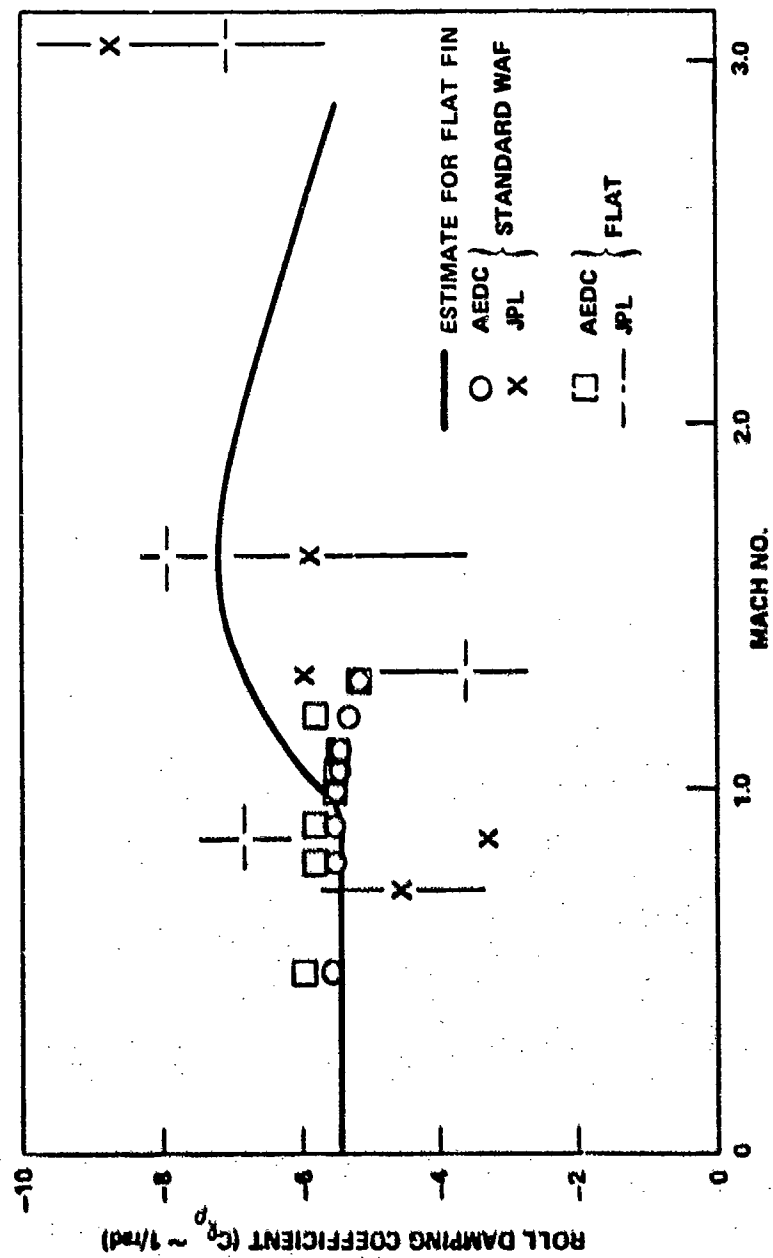


Figure 39. Comparison of roll damping for Flat and WAF.

IX. CONCLUSIONS

The general characteristics of a number of WAF's on a body of revolution at Mach numbers 0.3 to 3.0 have been presented. The effects of geometric and flow parameters are summarized in the following statements:

a) The static stability derivatives at $\alpha = 0$ of missiles with WAF's are essentially the same as with equivalent planar fins and may be estimated by using the flat fin techniques.

b) Drag of the WAF is larger than the flat fin with the same projected planform area. This increase is approximately a factor of 1.1, for the fins tested, which corresponds to the increase in frontal area of the WAF over the flat fin.

c) The WAF does induce roll moment to the missile at zero angle of attack and zero fin cant. This self-induced roll moment can change direction as a function of Mach number shown, from static data, to crossover near Mach 1.0 for smooth bodies. The parameter appearing to influence the subsonic roll moment most is the fin root chord length, indicating a fin-body juncture effect.

d) Step-downs on the afterbody, simulating a fin hinge recess, show additional crossover of the WAF-induced roll moment at supersonic Mach numbers from 1.2 to 3.0.

e) The WAF rolling moment variation with total missile angle of attack is small for absolute angles of attack less than 2° . Above 2° the rolling moment may deviate significantly from the zero angle of attack case depending upon fin geometry and Mach number.

f) Cross derivatives induced by the WAF do not appear to be significant at Mach numbers below 2.5. This may not be the case for Mach numbers above 2.5, for three-fin configurations, WAF configurations where fin opening directions are alternated, or higher angles of attack.

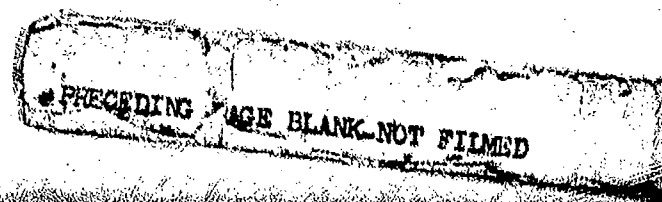
g) Accurate measurement of WAF rolling moment requires sensitive roll moment measurement instrumentation and small tolerance on the individual fin geometric incidence.

h) The WAF moments do not appear to be intolerable, and missile roll rates can be tailored by proper geometric design for many applications.

The summary of WAF aerodynamics presented in this report is believed to be adequate, in many cases, as preliminary estimates for aerodynamic design. In addition, the many parameters presented are for familiarization or as a guide for initial design and testing when WAF's are applied to specific designs. A complete summary of all static stability data obtained during this study are contained in a companion data report [14].

SYMBOLS

A	Reference area, $\pi D^2/4$
AR	Fin aspect ratio, $(b/2)^2 * S$
b	Fin total exposed span, 2 panels
C_{D_F}	Drag coefficient less base drag
C_{ℓ}	Rolling moment coefficient based on A*D
$C_{\ell \rho}$	Roll damping coefficient, $d C_{\ell}/d(\rho D/2V)$
C_N	Normal force coefficient
C_{N_α}	$d C_N/d\alpha$ at $\alpha = 0$
C_R	Fin root chord
C_T	Fin tip chord
C_y	Side force coefficient
D	Reference length-body diameter, 4.0 in.
L	Model total length, 40.0 in.
M	Mach number
P_t	Wind tunnel stagnation pressure
R_N	Reynolds number
S	Fin projected planform exposed area, $b/4*(C_R + C_T)$
t	Fin thickness
WAF	Wrap around fin
X_{cp}	Center of pressure, longitudinal
Y_{cp}	Fin spanwise center of pressure
α	Angle of attack
δ	Leading edge total included wedge angle (deg)
θ	Fin opening/closing angle (deg)
Λ	Leading edge sweep angle (deg)
ϕ	Roll attitude (deg)
TTCP	The Technical Cooperative Program Exterior Ballistics Panel-07



REFERENCES

1. Holmes, John E., Wrap-Around Fin (WAF) Aerodynamics, Paper 9th Navy Symposium Aeroballistics, Naval Ordnance Laboratory, Silver Spring, Maryland.
2. Dahlke, C. Wayne and Craft, J. C., Aerodynamic Characteristics of Wrap-Around Fins Mounted on Bodies of Revolution and Their Influence on the Missile Static Stability at Mach Numbers from 0.3 to 1.3, Vols. I and II, US Army Missile Command, Redstone Arsenal, Alabama, March 1972, Report No. RD-TM-72-1.
3. Dahlke, C. Wayne and Flowers, L. D., The Aerodynamic Characteristics of Wrap-Around Fins, Including Fold Angle, at Mach Numbers From 0.5 to 1.3, US Army Missile Command, Redstone Arsenal, Alabama, 20 December 1974, Report No. RD-75-19.
4. Dunkin, O. L., Influence of Curved-Fin Stabilizers on the Rolling Moment Characteristics of 10-Cal Missiles at Mach Numbers from 0.2 to 1.3, Propulsion Wind Tunnel Facility, Arnold Engineering Development Center, Air Force Systems Command, Arnold Air Force Station, Tennessee, October 1971, Report No. AEDC-TR-71-237.
5. Dahlke, C. Wayne and Craft, J. C., Static Aerodynamic Stability Characteristics of a Body of Revolution with Wrap-Around Fins at Mach Numbers from 0.5 to 1.3, US Army Missile Command, Redstone Arsenal, Alabama, June 1972, Report No. RD-TM-72-6.
6. Craft, J. C. and Skorupski, Jeff, Static Aerodynamic Stability Characteristics of Munitions Designs at Transonic Mach Numbers, US Army Missile Command, Redstone Arsenal, Alabama, February 1973, Report No. RD-73-3.
7. Dahlke, C. Wayne and Craft, J. C., Static Aerodynamic Stability Characteristics of Bodies of Revolution with Wrap-Around Fins at Mach Numbers from 1.6 to 2.86, US Army Missile Command, Redstone Arsenal, Alabama, September 1971, Report No. RD-TM-72-14.
8. Dahlke, C. Wayne and Flowers, L. D., The Aerodynamics Characteristics of Wrap-Around Fins, Including Fold Angle at Mach Numbers from 0.5 to 3.0, US Army Missile Command, Redstone Arsenal, Alabama, 15 November 1974, Report No. RD-75-15.
9. Spring, D. J., Static Stability and Roll Damping Characteristics for Several Curved and Planar Fin Configurations at Transonic Speeds, US Army Missile Command, Redstone Arsenal, Alabama, 24 September 1973, Report No. RD-73-32.

10. Featherstone, H. A., The Aerodynamic Characteristics of Curved Tail Fin, Convair/Pomona, Convair Division of General Dynamics Corporation, 26 September 1960, Report No. ERR-PO-019.
11. Dahlke, C. Wayne, Aerodynamics of Wrap-Around Fins, A Survey of the Literature, US Army Missile Command, Redstone Arsenal, Alabama, March 1971, Report No. RD-TR-71-7.
12. Stevens, F. L.; On, T. J.; and Clare, T. A., Wrap-Around Versus Cruciform Fin: Effect on Rocket Flight Performances, Naval Weapons Laboratory, Dahlgren, Virginia, August 1974, ARAA Paper 74-777.
13. Shadow, T. O., Transonic Static Stability and Roll-Damping Characteristics of a Directional Controlled Antitank Missile, Propulsion Wind Tunnel Facility, Arnold Engineering Development Center, Air Force Systems Command, Arnold Air Force Station, Tennessee, August 1973, Report No. AEDC-TR-73-131.
14. Humphery, J. A. and Dahlke, C. W. "A Summary of Aerodynamic Characteristics For Wrap Around Fins from Mach 0.3 to 3.0", US Army Missile Command, Redstone Arsenal, Alabama (in Preparation.)

BIBLIOGRAPHY

MICOM Wrap-Around Studies

1. Dahlke, C. Wayne, Aerodynamics of Wrap-Around Fins, A Survey of the Literature, US Army Missile Command, Redstone Arsenal, Alabama, March 1971, Report No. RD-TR-71-7.
2. Dahlke, C. Wayne, "A Review and Status of Wrap-Around Fin Aerodynamics," Volume I, Proceedings, 10th Navy Symposium on Aeroballistics, Naval Surface Weapons Center, Dahlgren Laboratory, Dahlgren, Virginia, 15-17 July 1975, p. 279.
3. Dahlke, C. Wayne, Experimental Investigation of Several Wrap-Around Fins on Bodies of Revolution From Mach 0.3 to 1.3, Data Report, US Army Missile Command, Redstone Arsenal, Alabama, September 1971, Report No. RD-TM-71-12.
4. Dahlke, C. Wayne and Craft, J. C., Aerodynamic Characteristics of Wrap-Around Fins Mounted on Bodies of Revolution and Their Influence on the Missile Static Stability at Mach Numbers from 0.3 to 1.3, Vols. I and II, US Army Missile Command, Redstone Arsenal, Alabama, March 1972, Report No. RD-TM-72-1.
5. Dahlke, C. Wayne and Craft, J. C., Static Aerodynamic Stability Characteristics of a Body of Revolution with Wrap-Around Fins at Mach Numbers from 0.5 to 1.3, US Army Missile Command, Redstone Arsenal, Alabama, June 1972, Report No. RD-TM-72-6.
6. Dahlke, C. Wayne and Craft, J. C., Static Aerodynamic Stability Characteristics of Bodies of Revolution with Wrap-Around Fins at Mach Numbers from 1.6 to 2.86, US Army Missile Command, Redstone Arsenal, Alabama, September 1972, Report No. RD-TM-72-14.
7. Dahlke, C. Wayne and Craft, J. C., The Effect of Wrap-Around Fins on Aerodynamic Stability and Rolling Moment Variations, US Army Missile Command, Redstone Arsenal, Alabama, July 1973, Report No. RD-73-17.
8. Dahlke, C. Wayne and Craft, J. C., "The Effect of Wrap-Around Fins on Rolling Moment and In-Flight Roll Rate Variations," Vol. II, Proceedings, Technical Briefings (Presented under the AEGIS of DEA-G-1060 at Eglin Air Force Base, Florida), US Ballistic Research Laboratories, Aberdeen Proving Ground, Maryland, 10-13 October 1972.
9. Dahlke, C. Wayne and Flowers, L. D., The Aerodynamic Characteristics of Wrap-Around Fins, Including Fold Angle at Mach Numbers From 0.5 to 1.3, US Army Missile Command, Redstone Arsenal, Alabama, December 1974, Report No. RD-75-19.

10. Dahlke, C. W. and Flowers, L. D., The Aerodynamics of Wrap-Around Fins, Including Fold Angle at Mach Numbers From 0.5 to 3.0, US Army Missile Command, Redstone Arsenal, Alabama, 15 November 1974, Report No. RD-75-15.

MICOM Reports — Projects and WAF Related

1. Craft, J. C., Summary of SMAWT Aerodynamics, US Army Missile Command, Redstone Arsenal, Alabama, 5 September 1973, Report No. RD-73-13.
2. Craft, J. C., Wind Tunnel Tests of Curved and Tangential Fin for Advanced LAW: Data Report, US Army Missile Command, Redstone Arsenal, Alabama, October 1969, Report No. RD-TM-69-12.
3. Craft, J. C. and Skorupski, J., Static Aerodynamic Stability Characteristics of Munitions Design at Transonic Mach Numbers, US Army Missile Command, Redstone Arsenal, Alabama, February 1973, Report No. RD-73-3.
4. Martin, T. A. and Spring, D. J., Wind Tunnel Results for the DCAT Missile at Mach Numbers from 0.64 to 2.50, US Army Missile Command, Redstone Arsenal, Alabama, 12 October 1973, Report No. RD-73-27.
5. Mottinger, T. A. and Washington, W. D., An Experimental Investigation of Low Aspect Ratio Fins Tested at Transonic Speeds on a Reflection Plane, US Army Missile Command, Redstone Arsenal, Alabama, July 1971, Report No. RD-TM-71-15.
6. Spring, D. J., Static Stability and Roll Damping Characteristics for Several Curved and Planar Fin Configurations at Transonic Speeds, US Army Missile Command, Redstone Arsenal, Alabama, 24 September 1973, Report No. RD-73-23.

MICOM Contract Reports

1. Dunkin, O. L., Aerodynamic Characteristics of Curved Fins with Swept and Unswept Leading Edges and Their Influence on Missile Static Stability at Mach Numbers from 0.5 to 1.3, Arnold Engineering Development Center, Arnold Air Force Station, Tennessee, May 1972, Report No. AEDC-TR-72-65 (AD894217L).
2. Dunkin, O. L., Effects of Fin Folding Angle and Leading Edge Sweep Angle on the Aerodynamic Characteristics of Missiles Equipped with Wrap-Around Fins at Mach Numbers from 0.5 to 1.3, Arnold Engineering Development Center, Arnold Air Force Station, Tennessee, November 1973, Report No. AEDC-TR-73-191.

3. Dunkin, O. L., Influence of Curved-Fin Stabilizers on the Rolling-Moment Characteristics of 10-Cal Missiles at Mach Numbers from 0.2 to 1.3, Propulsion Wind Tunnel Facility, Arnold Engineering Development Center, Air Force Systems Command, Arnold Air Force Station, Tennessee, October 1971, Report No. AEDC-TR-71-237.
4. Dunkin, O. L. and German, R. C., Aerodynamic Characteristics of Curved and Planar Fins and Their Influence on Missile Static Stability at Mach Numbers from 0.3 to 1.3, Arnold Engineering Development Center, Air Force Systems Command, Arnold Air Force Station, Tennessee, September 1971, Report No. AEDC-TR-71-201.
5. Hube, F. K., Aerodynamic Characteristics of a Fluidic-Controlled Antitank Missile at Mach Numbers From 2.0 to 3.0, Von KA'RMA'N Gas Dynamics Facility, Arnold Engineering Development Center, Air Force Systems Command, Arnold Air Force Station, Tennessee, August 1971, Report No. AEDC-TR-71-158.
6. Shadow, T. O., Transonic Static Stability and Roll-Damping Characteristics of a Directional Controlled Antitank Missile, Propulsion Wind Tunnel Facility, Arnold Engineering Development Center, Air Force Systems Command, Arnold Air Force Station, Tennessee, August 1973, Report No. AEDC-TR-73-131.
7. Whoric, J. M., Aerodynamic Characteristics of a Fluidic-Controlled Antitank Missile With Curved Fins at Mach Numbers From 0.2 to 1.3, Propulsion Wind Tunnel Facility, Arnold Engineering Development Center, Air Force Systems Command, Arnold Air Force Station, Tennessee, July 1971, Report No. AEDC-TR-71-116.
8. Whoric, J. M., Aerodynamic Characteristics of Several Low Aspect Ratio Stabilizer Fins at Mach Numbers from 0.8 to 1.3, Propulsion Wind Tunnel Facility, Arnold Engineering Development Center, Air Force Systems Command, Arnold Air Force Station, Tennessee, September 1972, Report No. AEDC-TR-72-143, AFATL-TR-72-189.

WAF Reports - Government Other than MICOM

1. Ailor, W. H. III, Supersonic Aerodynamic Characteristics of a Wrap-Around Folding Fin, Naval Ordnance Station, Indian Head, Maryland, 10 June 1971, Report No. 337.
2. Blackaby, J. R., and Watson, E. C., An Experimental Investigation at Low Speeds of the Effects of Lip Shape on the Drag and Pressure Recovery of a Nose Inlet in a Body of Revolution, April 1954, NACA Technical Note 3170.
3. Butler, R. W., Evaluation of the Pressure Distribution on the Fins of a Wrap-Around Fin Model at Supersonic and Transonic Mach Numbers, Propulsion Wind Tunnel Facility, Arnold Engineering Development Center, Air Force Systems Command, Arnold Air Force Station, Tennessee, December 1971, Report No. AEDC-TR-71-273.

4. Daniels, P. and Hardy, S. R., Roll Rate Stabilization of a Missile Configuration with Wrap-Around Fins in Incompressible Flow, Naval Surface Weapons Center, Dahlgren, Virginia, December 1975, NSWC/DL TR-3346.
5. Featherstone, H. A., The Aerodynamic Characteristics of Curved Tail Fin, Convair/Pomona, Convair Division of General Dynamics Corporation, 26 September 1960, Report No. ERR-PO-019.
6. Gauzza, H. J., Static Stability Test of Tangent and Wrap-Around Fin Configuration at Supersonic Speeds, US Naval Ordnance Laboratory, White Oak, Maryland, 17 January 1955, NAVORD Report No. 3743.
7. Holmes, John E., Wrap-Around Fin (WAF) Aerodynamics, Paper, 9th Navy Symposium Aeroballistics, Naval Ordnance Laboratory, Silver Spring, Maryland.
8. Holmes, John E., Wrap-Around Fin (WAF) Pressure Distribution, Naval Ordnance Laboratory, White Oak, Silver Spring, Maryland, 1 October 1973, NOLTR Report No. 73-157.
9. Stevens, F. L., Analysis of the Linear Pitching and Yawing Motion of Curved-Finned Missiles, Naval Weapons Laboratory, Dahlgren, Virginia, October 1973, NWL Report No. TR-2989.
10. Stevens, F. L.; On, T. J.; and Clare, T. A., Wrap-Around Versus Cruciform Fin: Effect on Rocket Flight Performances, Naval Weapons Laboratory, Dahlgren, Virginia, August 1974, ARAA Paper 74-777.
11. Weaver, R. W., The Aerodynamic Characteristics of Wrap-Around Fins for a Rocket Improvement Program, Jet Propulsion Laboratory, 30 June 1969, JPL Document 650-68.

Foreign National WAF Reports

1. Carrington, B. L.; Hurdle, C. V.; and Faneett, R. K., Wrap-Around Fins - The Results of a Supersonic Parametric Study, Royal Armament Research and Development Establishment, Fort Halstead Seven Oaks Kent England, 9th Meeting of the TTCP Exterior Ballistics Panel 0-7, DREV, Quebec, September 1971.
2. Dixon, R. C., Wind Tunnel Test of a Model Employing Wrap-Around Fins, National Aeronautical Establishment, High Speed Aerodynamic Section, National Research Council of Canada, Ottawa, March 1972, Report No. 5X5/0058.

3. Dixon, R. C., Wind Tunnel Test of a Model Employing Wrap-Around Fins, National Aeronautical Establishment, High Speed Aerodynamic Section, National Research Council of Canada, Ottawa, Addendum to Report 5X5/0058, October 1972.
4. Robinson, M. L. and Fenton, C. E., Static Aerodynamic Characteristics of a Wrap-Around Fin Configuration with Small Rolling Moments at Low Incidence, Department of Supply, Australian Defense Scientific Service, Weapons Research Establishment (No Number), The Director, Weapons Research Establishment, Box 1424H, G.P.O. Adelaide, South Australia, 5001.
5. Wingrove, J. S., Analysis of Errors and Zero Incidence Rolling Moments, British Aircraft Corporation Limited, Guided Weapons Division: Bristol Works, Curved Aerodynamic Surfaces, Study Note No. 1, June 1972, Report No. ST-7376.
6. Wingrove, J. S., Analysis of Zero Incidence Spin Rates and Roll Damping Coefficients, British Aircraft Corporation Limited, Guided Weapons Division: Bristol Works, Curved Aerodynamic Surfaces, Study Note No. 2, August 1972, Report No. 7645.